



Evidence for Higgs boson decays to a low-mass dilepton system and a photon in pp collisions at $\sqrt{s} = 13$ TeV with the ATLAS detector

The ATLAS Collaboration*



ARTICLE INFO

Article history:

Received 19 March 2021

Received in revised form 11 May 2021

Accepted 25 May 2021

Available online 31 May 2021

Editor: M. Doser

ABSTRACT

A search for the Higgs boson decaying into a photon and a pair of electrons or muons with an invariant mass $m_{\ell\ell} < 30$ GeV is presented. The analysis is performed using 139 fb^{-1} of proton–proton collision data, produced by the LHC at a centre-of-mass energy of 13 TeV and collected by the ATLAS experiment. Evidence for the $H \rightarrow \ell\ell\gamma$ process is found with a significance of 3.2 over the background-only hypothesis, compared to an expected significance of 2.1 for the Standard Model prediction. The best-fit value of the signal-strength parameter, defined as the ratio of the observed signal yield to the one expected in the Standard Model, is $\mu = 1.5 \pm 0.5$. The Higgs boson production cross-section times the $H \rightarrow \ell\ell\gamma$ branching ratio for $m_{\ell\ell} < 30$ GeV is determined to be $8.7^{+2.8}_{-2.7} \text{ fb}$.

© 2021 The Author. Published by Elsevier B.V. This is an open access article under the CC BY license (<http://creativecommons.org/licenses/by/4.0/>). Funded by SCOAP³.

1. Introduction

In July 2012, the ATLAS and CMS Collaborations at the CERN Large Hadron Collider (LHC) announced the discovery of a new particle with a mass of approximately 125 GeV [1,2]. The observed properties of the particle, such as its couplings to Standard Model (SM) elementary particles, its spin and its parity, are so far consistent with the predictions for the SM Higgs boson [3–7].

Measurements of rare decays of the Higgs boson, such as $H \rightarrow \ell\ell\gamma$ where ℓ is an electron or muon, can probe coupling modifications introduced by possible extensions to the SM [8]. In addition, such three-body Higgs boson decays can be used to probe CP -violation in the Higgs sector [9,10].

Multiple processes contribute to the $H \rightarrow \ell\ell\gamma$ decay: Dalitz decays involving a Z boson or a virtual photon (γ^*) (Fig. 1(a–c)), as well as the decay of the Higgs boson to two leptons and a photon from final-state radiation (FSR) (Fig. 1(d)). Their respective fractions depend on the invariant mass of the dilepton pair, $m_{\ell\ell}$. In this analysis only low-mass dilepton pairs with $m_{\ell\ell} < 30$ GeV are considered. This region is completely dominated by the decay through γ^* [8,11,12]. The contributions of the other processes and interferences are negligible.

Based on a data sample of proton–proton (pp) collisions at $\sqrt{s} = 13$ TeV with an integrated luminosity of 35.9 fb^{-1} , the CMS Collaboration reported a 95% CL upper limit on the production cross-section times branching ratio for the low- $m_{\mu\mu}$ $H \rightarrow \mu\mu\gamma$ process of 4.0 times the SM prediction [13]. In addition, both the ATLAS and CMS Collaborations carried out searches at

$\sqrt{s} = 13$ TeV for the closely related $H \rightarrow Z\gamma$ process [13,14]. The CMS Collaboration also searched for the low- $m_{\ell\ell}$ $H \rightarrow \ell\ell\gamma$ process in the dimuon and dielectron channels in pp collisions at $\sqrt{s} = 8$ TeV [15].

This paper describes a search for $H \rightarrow ee\gamma$ and $H \rightarrow \mu\mu\gamma$ decays with $m_{\ell\ell} < 30$ GeV. When the invariant mass of the two electrons is low and the transverse momentum of the dielectron system is high, their electromagnetic showers can overlap in the calorimeter. Therefore, the search for $ee\gamma$ final states requires the development of dedicated electron trigger and identification algorithms.

The search uses pp collision data at $\sqrt{s} = 13$ TeV recorded with the ATLAS detector during Run 2 of the LHC between 2015 and 2018, corresponding to a total integrated luminosity of 139 fb^{-1} . The sensitivity of the search is enhanced by dividing the selected events into mutually exclusive categories, according to the event topology and lepton flavour. The dominant background is the irreducible non-resonant production of $\ell\ell\gamma$. After event categorisation, the signal yield is extracted by a simultaneous fit of parametric functions to the reconstructed $\ell\ell\gamma$ invariant mass ($m_{\ell\ell\gamma}$) distributions in all categories.

2. ATLAS detector

The ATLAS detector [16] covers nearly the entire solid angle around the collision point.¹ It consists of an inner tracking de-

* E-mail address: atlas.publications@cern.ch.

¹ The ATLAS experiment uses a right-handed coordinate system with its origin at the nominal interaction point (IP) in the centre of the detector and the z-axis along the beam pipe. The x-axis points from the IP to the centre of the LHC ring, and the y-axis points upward. Cylindrical coordinates (r, ϕ) are used in the transverse

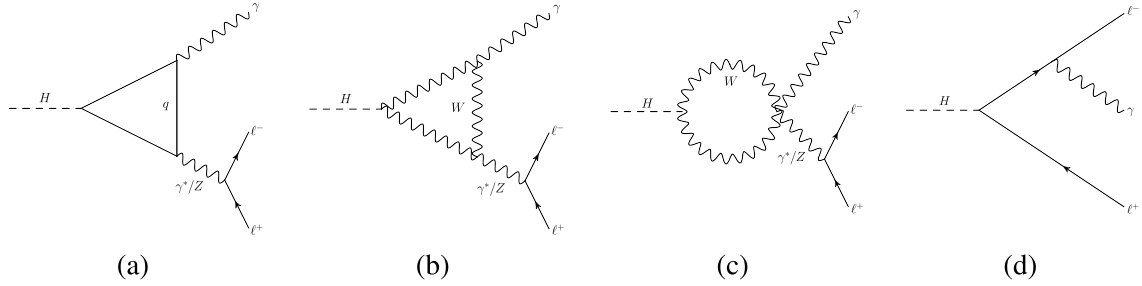


Fig. 1. Representative Feynman diagrams of the $H \rightarrow \ell\ell\gamma$ process.

tector (ID) surrounded by a thin superconducting solenoid providing a 2 T axial magnetic field, electromagnetic (EM) and hadron calorimeters, and a muon spectrometer (MS). The ID covers the pseudorapidity range $|\eta| < 2.5$. It consists of silicon pixel, silicon microstrip, and transition radiation tracking detectors. The silicon pixel detector provides up to four measurements per track. The insertable B-layer (IBL) [17,18] constitutes the innermost layer at a radius of 33.3 mm. It surrounds the beam pipe, which has an inner radius of 23.5 mm. Lead/liquid-argon (LAr) sampling calorimeters provide EM energy measurements with high granularity. A steel/scintillator-tile hadron calorimeter covers the central pseudorapidity range ($|\eta| < 1.7$). The endcap and forward regions are instrumented with LAr calorimeters for both the EM and hadronic energy measurements up to $|\eta| = 4.9$. For $|\eta| < 2.5$, the EM calorimeter is divided into three longitudinal layers, which are finely segmented in η and ϕ , particularly in the first layer. This segmentation allows the measurement of the lateral and longitudinal shower profile, and the calculation of shower shapes [19] used for particle identification and background rejection. The longitudinal segmentation of the EM calorimeter is also exploited to calibrate the energy response of electron and photon candidates [19]. The MS comprises separate trigger and high-precision tracking chambers measuring the deflection of muons in a magnetic field generated by superconducting air-core toroids. The precision chamber system covers the region $|\eta| < 2.7$ with three layers of monitored drift tubes, complemented by cathode-strip chambers in the forward region, where the background is highest. The muon trigger system covers the range $|\eta| < 2.4$ with resistive-plate chambers in the barrel, and thin-gap chambers in the endcap regions.

A two-level trigger system [20] was used during the $\sqrt{s} = 13$ TeV data-taking period. The first-level trigger (L1) is implemented in hardware and uses a subset of the detector information. This is followed by a software-based high-level trigger which runs algorithms similar to those in the offline reconstruction software, reducing the event rate to approximately 1 kHz from the maximum L1 rate of 100 kHz.

3. Data and simulated event samples

The analysed pp collision data correspond to the full recorded LHC Run-2 data set at $\sqrt{s} = 13$ TeV with an integrated luminosity of 139 fb^{-1} after data quality requirements [21]. The events were collected with a combination of single-lepton, dilepton, diphoton, and lepton+photon triggers. Standard electron triggers, which require narrow, isolated EM energy clusters, are efficient if the two electrons in the event have a very small angular separation ΔR_{ee} ,

as the two electrons produce a cluster that is similar to that of a single electron. For $\Delta R_{ee} > 0.1$, two separate EM clusters are typically produced. For the 2017 and 2018 data-taking periods, a dedicated trigger was introduced which requires at least one photon with $p_T > 35 \text{ GeV}$ and at least one EM cluster with $p_T > 25 \text{ GeV}$ matched to at least one ID track. The EM cluster must have low hadronic leakage, but no requirement is imposed on the width of the shower, which allows this new trigger to recover a significant fraction of the signal with $0.025 < \Delta R_{ee} < 0.1$. More details are provided in Ref. [22]. The overall trigger efficiencies for the $H \rightarrow ee\gamma$ and $H \rightarrow \mu\mu\gamma$ processes are 98% and 96%, respectively (97% combined), relative to the event selection discussed in Section 5. The uncertainty in the trigger efficiency is negligible.

Samples of simulated Monte Carlo (MC) events are crucial for the optimisation of the search strategy and the modelling of the signal and background processes. Simulated $H \rightarrow \gamma^*\gamma \rightarrow \ell\ell\gamma$ signal and $H \rightarrow \gamma\gamma$ background events are used to parameterise these processes, and simulated non-Higgs $\ell\ell\gamma$ events are used to choose analytic functional forms to describe the non-resonant background. The generated MC events, unless stated otherwise, were processed with the full ATLAS detector simulation [23] based on GEANT4 [24]. The effect of multiple pp interactions in the same and neighbouring bunch crossings (pile-up) was included by overlaying minimum-bias events simulated with PYTHIA 8.186 [25] using the NNPDF2.3LO parton distribution function (PDF) set [26] and the A3 set [27] of tuned parameters. The MC events were weighted to reproduce the distribution of the number of interactions per bunch crossing observed in the data.

Higgs boson production in the gluon–gluon fusion (ggF) and vector-boson fusion (VBF) production modes, as well as in quark-initiated associated production with a W or Z boson ($q\bar{q}/qg \rightarrow VH$) or with two top quarks ($t\bar{t}H$) was modelled with the PowHEG-Box v2 MC event generator [28–32]. PowHEG-Box v2 was interfaced with PYTHIA 8 [25] to simulate the $H \rightarrow \gamma^*\gamma \rightarrow \ell\ell\gamma$ and $H \rightarrow \gamma\gamma$ decays. PYTHIA also provides parton showering, hadronisation and the underlying event. The PDF4LHC15 PDF set [33] was used, except for $t\bar{t}H$, where the NNPDF3.0nlo PDF set [26] was used. For the ggF process, the PowHEG NNLOPS program [34,35] achieves next-to-next-to-leading-order (NNLO) accuracy in QCD for inclusive observables after reweighting the Higgs boson rapidity spectrum [36]. The simulation reaches next-to-leading-order (NLO) accuracy in QCD for the VBF, VH , and $t\bar{t}H$ processes. For VH , the MiNLO technique [37–39] was applied. No simulated samples are available for gluon-initiated associated production with a Z boson ($gg \rightarrow ZH$) and associated production with two b -quarks (bbH). Their minor contribution, 1% of the expected Higgs boson production, is modelled using the acceptances from the $q\bar{q}/qg \rightarrow ZH$ and ggF samples, respectively.

Alternative $H \rightarrow \gamma\gamma$ samples are considered for the ggF and VBF processes, where HERWIG 7 [40] was used instead of PYTHIA 8 to provide parton showering. Weights were calculated by comparing the generator-level Higgs boson transverse momentum and jet distributions in these samples with the distributions obtained from

plane. The polar angle (θ) is measured from the positive z -axis and the azimuthal angle (ϕ) is measured from the positive x -axis in the transverse plane. The pseudorapidity is defined as $\eta = -\ln \tan(\theta/2)$. Angular distance is measured in units of $\Delta R = \sqrt{(\Delta\eta)^2 + (\Delta\phi)^2}$.

the nominal $H \rightarrow \gamma\gamma$ samples. The weights are applied to the $H \rightarrow \gamma^*\gamma \rightarrow \ell\ell\gamma$ ggF and VBF samples to estimate the effect of varying the parton shower and underlying event.

The mass of the Higgs boson was set in the simulation to $m_H = 125$ GeV and its width to $\Gamma_H = 4.1$ MeV [41]. The Higgs mass peak position in the simulation was corrected to account for the small difference relative to the measured value of 125.09 GeV [42] (see Section 6); otherwise the effect on the kinematics is neglected.

The signal and $H \rightarrow \gamma\gamma$ samples were normalised with the best available theoretical calculations of the corresponding SM production cross-sections at $m_H = 125.09$ GeV, which are available at next-to-next-to-next-to-leading order (N3LO) in QCD with NLO electroweak (EW) corrections for ggF [41,43–54], at approximate NNLO in QCD with NLO EW corrections for VBF [41,55–57], at NNLO in QCD with NLO EW corrections for $q\bar{q}/qg \rightarrow VH$ [41,58–65] and at NLO in QCD with NLO electroweak corrections for $t\bar{t}H$ [41,66–69]. The accuracy of the calculation is NNLO in QCD for bbH [70–72], and NLO in QCD with next-to-leading-logarithm (NLL) corrections for $gg \rightarrow ZH$ [41,61].

There are multiple calculations of the $H \rightarrow \ell\ell\gamma$ branching ratios for different slices of phase space [8,11,12,73–76]. The $H \rightarrow \ell\ell\gamma$ branching ratios used in this analysis are $\mathcal{B}(H \rightarrow ee\gamma) = 7.20 \times 10^{-5}$ and $\mathcal{B}(H \rightarrow \mu\mu\gamma) = 3.42 \times 10^{-5}$, as estimated with PYTHIA 8 for $m_{ee} < 30$ GeV. Their sum corresponds to $\sim 5\%$ of the $H \rightarrow \gamma\gamma$ branching ratio. When extrapolated to a common phase space, the PYTHIA 8 estimate agrees with the predictions of Refs. [74,76] within a relative difference of 3%. Currently, no theoretical uncertainty calculation exists for the low- m_{ee} $H \rightarrow \ell\ell\gamma$ branching ratio. Therefore, the theoretical uncertainties in the $H \rightarrow \gamma\gamma$ and $H \rightarrow Z\gamma$ branching ratios are considered [12], and the larger of the two uncertainties is used, which corresponds to the 5.8% relative uncertainty in the $H \rightarrow Z\gamma$ branching ratio [41].

The background originates mainly from non-resonant $\ell\ell\gamma$ production. Events were simulated with the SHERPA 2.2.8 [77] generator based on LO matrix elements for $\ell\ell\gamma$ production with up to three additional partons and using the NNPDF3.0 PDF set [78]. The SHERPA simulation includes parton shower, fragmentation and underlying-event modelling. As the statistical uncertainties in the simulated $\ell\ell\gamma$ background samples are a limiting factor when studying the background modelling at the level required by the small signal-to-background ratio, a procedure was developed to generate significantly larger samples. These are based on events generated using the SHERPA 2.2.8 configuration described above with object efficiencies approximated by parameterisations rather than using the full ATLAS detector simulation and reconstruction software. The parameterisations, extracted from fully simulated MC samples, reproduce the reconstruction and selection efficiencies of detector-level objects via event weighting. Comparisons with a sample that underwent the full ATLAS detector simulation, and whose effective luminosity is greater than the data luminosity, show good agreement within the statistical uncertainties.

4. Object selection

Events are required to have a collision vertex associated with at least two tracks with transverse momentum $p_T > 0.5$ GeV each. In the case of multiple vertices, the vertex with the largest $\sum p_T^2$ of the associated tracks is considered to be the primary vertex.

Muon candidates are obtained by matching high-quality tracks in the MS and ID. Standalone MS tracks are used to extend the muon reconstruction beyond the ID acceptance to $2.5 < |\eta| < 2.7$. Muon candidates are required to satisfy the *medium* identification criteria [79,80], be within $|\eta| < 2.7$ and have $p_T > 3$ GeV. Muon candidates with an associated ID track must be matched to the primary vertex by having a longitudinal impact parameter Δz_0 that satisfies $|\Delta z_0 \cdot \sin\theta| < 0.5$ mm, where θ is the polar angle of the

track. The significance of the transverse impact parameter d_0 calculated relative to the measured beam-line position is required to be $|d_0|/\sigma_{d_0} < 3$, where σ_{d_0} is the uncertainty in d_0 . A subset of the muon candidates are also required to be isolated from additional activity in the tracking detector and in the calorimeters, using a loose isolation selection [79,80]. The efficiency of the muon reconstruction and identification, as well as the momentum calibration, including the associated systematic uncertainties, is estimated as described in Refs. [79,80].

Photon and electron candidates are reconstructed from energy clusters in the calorimeters which are formed using an algorithm based on dynamical, topological cell-clustering [19]. Candidates in the transition region between the barrel and endcap EM calorimeters, $1.37 < |\eta| < 1.52$, are excluded. The performance of the electron and photon reconstruction, including the associated systematic uncertainties, is studied in Ref. [19].

Photon candidates can be either unconverted or converted. In the latter case, a track or conversion vertex is matched to the EM cluster. Photon candidates are required to satisfy $p_T > 20$ GeV and $|\eta| < 2.37$, and pass the *tight* identification requirements [19,81] as well as a loose isolation selection [19].

The energy of the EM clusters associated with the photon and electron candidates is corrected in successive steps using a combination of simulation-based and data-driven correction factors [19]. The simulation-based calibration regression is optimised separately for electrons, unconverted photons and converted photons. The resolution of the energy response is corrected in the simulation to match the resolution observed in data using $Z \rightarrow ee$ events, by smearing the electron energy such that the width of the simulated Z boson peak matches the width observed in data.

Because of the event kinematics of the signal process, it is common for the energy deposits of the two electrons in the EM calorimeter to be reconstructed as a single cluster. Therefore, two types of electron candidates are defined, each with its own selection criteria: one in which a topological cluster of energy deposits is associated with one selected ID track (*resolved* electron [82]), representing a single electron, and one in which a topological cluster is associated with two selected ID tracks (*merged ee*), representing a merged electron pair. Each ID track considered must satisfy $|\Delta z_0 \cdot \sin\theta| < 0.5$ mm and $|d_0|/\sigma_{d_0} < 5$. Resolved electron candidates must satisfy the *medium* likelihood-based identification criteria [19,82], have $p_T > 4.5$ GeV and be within $|\eta| < 2.47$. A subset of the resolved electron candidates are also required to pass a loose isolation requirement [19].

ID tracks considered for merged electrons must have opposite charge, $p_T > 5$ GeV, $|\eta| < 2.5$, and at least seven hits in the pixel and microstrip detectors combined. To suppress backgrounds from converted photons, tracks must also have a hit in the innermost pixel layer, and merged-electron candidates are rejected if they match a conversion vertex with a radius larger than 20 mm whose momentum agrees better with the cluster energy than the momentum of the track that geometrically matches the cluster best. Because the kinematic behaviour of merged electrons in the calorimeter most closely resembles a photon converting in the material close to the interaction vertex, the energy of the merged-ee object is calibrated as a converted photon with a conversion radius set to $r_{\text{conv}} = 30$ mm calculated relative to the measured beam-line position. As presented in Fig. 2(a), this treatment is found to induce minimal bias in the dielectron energy measurement. To cover remaining differences between the simulated detector response to converted photons and merged-ee objects, the difference between the squares of the energy resolutions for converted photons and merged-ee objects in the MC simulation is treated as the square of an additional energy resolution uncertainty. The four-momentum of the merged-ee candidate is constructed using the calibrated en-

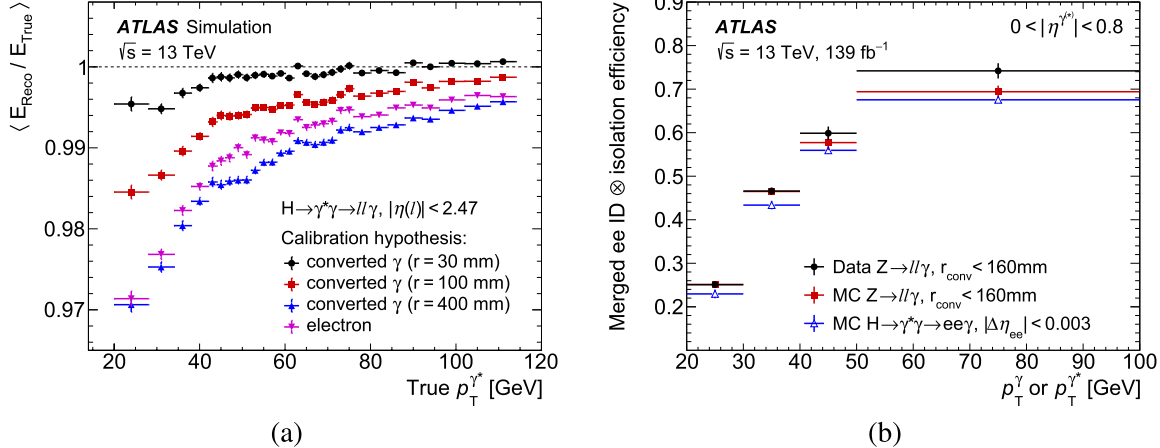


Fig. 2. (a) Ratio of reconstructed to true merged-ee energy in simulated $H \rightarrow \gamma^* \gamma \rightarrow ee\gamma$ events as a function of the true merged-ee p_T for several energy calibration techniques. The merged-ee object is calibrated as a photon with a conversion radius of 30 mm (black circles, analysis choice), 100 mm (red squares), and 400 mm (blue upward triangles) or as an electron (purple downward triangles). (b) Combined merged-ee identification and isolation efficiency extracted from $Z \rightarrow ll\gamma$ events with a photon that converts at a radius of $r_{\text{conv}} < 160$ mm. The efficiencies are shown for photons with $|\eta| < 0.8$ as a function of p_T . Data (black circles) are compared with efficiencies in simulated $Z \rightarrow ll\gamma$ events (red squares). The resulting efficiencies are also compared with efficiencies in simulated $H \rightarrow \gamma^* \gamma \rightarrow ee\gamma$ events (blue triangles). On all points, the vertical error bars indicate the statistical uncertainties.

ergy and the direction and invariant mass obtained from the vertex reconstructed from the two electron-track candidates [83].

Merged-ee candidates are required to have $|\eta| < 2.37$ (excluding $1.37 < |\eta| < 1.52$) and $p_T > 20$ GeV, and satisfy dedicated identification requirements, as the standard electron criteria have a low efficiency for objects with closely spaced energy deposits or broader EM showers. For the merged-ee identification, a multivariate discriminator is trained to separate the $\gamma^* \rightarrow ee$ signal objects from jets or single electrons. The input variables for the training include shower shape variables [82], the information provided by the transition radiation tracker [84], and the kinematic information from the cluster and ID tracks. Merged-ee candidates are also required to pass a tight isolation requirement [19]. A combined efficiency of $\sim 50\%$ for the merged-ee identification and isolation is achieved for $H \rightarrow \gamma^* \gamma \rightarrow ee\gamma$ events. Since photons with a relatively small conversion radius offer a signature similar to that of merged-ee objects, the merged-ee identification and isolation efficiency is measured in data using a tag-and-probe method with FSR photons from Z boson radiative decays ($Z \rightarrow ll\gamma$). Candidate $Z \rightarrow ll\gamma$ events are selected similarly to those in Ref. [81]. Only two-track converted photons with $r_{\text{conv}} < 160$ mm, corresponding to conversions inside the silicon pixel detector volume, are considered. The $Z \rightarrow ll\gamma$ and background yields are estimated from a fit to the $m_{ll\gamma}$ distribution in data. The extracted efficiencies are compared with the efficiencies estimated from simulated $Z \rightarrow ll\gamma$ events as shown in Fig. 2(b) for photons with $|\eta| < 0.8$. The resulting p_T - and η -dependent data/simulation scale factors are between 0.9 and 1.1 and are used to correct the identification and isolation efficiencies of the simulated $H \rightarrow \gamma^* \gamma \rightarrow ee\gamma$ events. The statistical uncertainties of the scale factors are taken into account. In addition, a systematic uncertainty is assessed for the background modelling by varying the selection criteria of the $m_{ll\gamma}$ background template. The total uncertainty reaches 2% for $20 < p_T < 30$ GeV and 9% for $p_T > 50$ GeV. Fig. 2(b) also shows a comparison of the extracted efficiencies with efficiencies in simulated $H \rightarrow \gamma^* \gamma \rightarrow ee\gamma$ events where an additional generator-level requirement of $|\Delta\eta_{ee}| < 0.003$ is used. This requirement is applied in order to better match the signal signature to the converted photon signature in the detector; approximately 70% of the merged-ee objects in the signal sample pass it. The efficiencies of converted photons and the merged-ee objects agree within 10%

for $p_T < 30$ GeV and within 5% for $p_T > 30$ GeV in the entire η range.

Jets are reconstructed from topological clusters [85] using the anti- k_t algorithm [86] with a radius parameter of 0.4 and are required to have $p_T > 20$ GeV and $|\eta| < 4.4$. Jets produced in pile-up interactions are suppressed by requiring that those with $p_T < 60$ GeV and $|\eta| < 2.4$ pass a selection based on a jet vertex tagging algorithm [87].

5. Event selection

Candidate $H \rightarrow \gamma^* \gamma \rightarrow ll\gamma$ events must have at least one reconstructed photon, and at least one opposite-charge, same-flavour pair of leptons (muons or resolved electrons) or one merged-ee object. One of the muons (resolved electrons) in the lepton pair must have $p_T > 11$ (13) GeV, to match the p_T thresholds used in the dilepton triggers. As discussed above, the merged-ee p_T is required to be larger than 20 GeV. If the leading photon overlaps with one of the EM clusters (resolved electrons or merged-ee) forming the γ^* candidate within $\Delta R < 0.02$, the photon is discarded and the next-highest- p_T photon is considered. No isolation requirement is applied to the subleading lepton (muon or resolved electron) as it is within the isolation cone of the leading lepton in the majority of events. Additionally, if the subleading lepton (muon or electron) falls within the isolation cone of the leading lepton, it is not included in the calculation of the isolation variable.

Muon pairs are given the highest priority if there are lepton pairs of different flavours in one event. If no opposite-charge muon pair satisfying the requirements above is found, the electron-pair candidates are considered. The resolved electron pair or merged-ee object with the highest vector-sum of the p_T of the associated ID tracks is selected.

In order to suppress events arising from FSR processes, events are rejected if the photon is within a $\Delta R = 0.4$ cone around either of the selected leptons. If the axis of a jet is within $\Delta R = 0.4$ of the photon or a muon, or within $\Delta R = 0.2$ of an electron (merged or resolved), the jet is discarded. However, if the electron-jet angular separation is $0.2 < \Delta R < 0.4$, the electron and therefore the event is discarded.

To suppress events involving Z boson decays, the dilepton invariant mass must satisfy $m_{ll} < 30$ GeV. To remove $J/\psi \rightarrow ll$ production, events with a dimuon (dielectron) invariant mass in

Table 1

Number of data events selected in each analysis category in the $m_{\ell\ell\gamma}$ mass range of 110–160 GeV. In addition, the following numbers are given: number of $H \rightarrow \gamma^*\gamma \rightarrow \ell\ell\gamma$ events in the smallest $m_{\ell\ell\gamma}$ window containing 90% of the expected signal (S_{90}), the non-resonant background in the same interval (B_{90}^N) as estimated from fits to the data sidebands using the background models described in Section 6, the resonant background in the same interval ($B_{H\rightarrow\gamma\gamma}$), the expected signal purity $f_{90} = S_{90}/(S_{90} + B_{90})$, and the expected significance estimate defined as $Z_{90} = \sqrt{2((S_{90} + B_{90}) \ln(1 + S_{90}/B_{90}) - S_{90})}$ where $B_{90} = B_{90}^N + B_{H\rightarrow\gamma\gamma}$. $B_{H\rightarrow\gamma\gamma}$ is only relevant for the electron categories and is marked as “–” otherwise.

Category	Events	S_{90}	B_{90}^N	$B_{H\rightarrow\gamma\gamma}$	f_{90} [%]	Z_{90}
ee resolved VBF-enriched	10	0.4	1.6	0.009	20	0.3
ee merged VBF-enriched	15	0.8	2.0	0.07	27	0.5
$\mu\mu$ VBF-enriched	33	1.3	5.9	–	18	0.5
ee resolved high- p_T	86	1.1	12	0.02	9	0.3
ee merged high- p_T	162	2.5	18	0.2	12	0.6
$\mu\mu$ high- p_T	210	4.0	34	–	11	0.7
ee resolved low- p_T	3713	22	729	0.5	2.9	0.8
ee merged low- p_T	5103	29	942	2	3.0	1.0
$\mu\mu$ low- p_T	9813	61	1750	–	3.4	1.4

the range $2.9 < m_{\mu\mu} < 3.3$ GeV ($2.5 < m_{ee} < 3.5$ GeV) are excluded. Similarly, events with a dimuon (dielectron) invariant mass in the range $9.1 < m_{\mu\mu} < 10.6$ GeV ($8.0 < m_{ee} < 11.0$ GeV) are rejected to avoid $\Upsilon(N)$ → $\ell\ell$ contamination.

The invariant mass of the $\ell\ell\gamma$ system is required to satisfy $110 < m_{\ell\ell\gamma} < 160$ GeV. Additionally, both the photon and dilepton momenta must satisfy $p_T > 0.3 \cdot m_{\ell\ell\gamma}$.

The selected events are classified into mutually exclusive categories, depending on the lepton types and event topologies. The VBF-enriched categories, which have the best expected signal-to-background ratio, but the lowest event count, are defined as follows. Events must contain at least two jets with $p_T > 25$ GeV. If the leading or subleading jet is a forward jet (defined as a jet with $|\eta| > 2.5$), it is required to have $p_T > 30$ GeV to suppress jets originating from pile-up. In addition, the invariant mass of the two leading jets, m_{jj} , must be greater than 500 GeV, and the pseudo-rapidity separation between the two leading jets, $|\Delta\eta_{jj}|$, greater than 2.7. The quantity $|\eta_{\ell\ell\gamma} - 0.5(\eta_{j1} + \eta_{j2})|$ [88] is required to be less than 2.0, where $\eta_{\ell\ell\gamma}$ is the pseudorapidity of the $\ell\ell\gamma$ system and η_{j1} (η_{j2}) is the pseudorapidity of the leading (subleading) jet. The selected leptons and the photon must be separated from the two jets by $\Delta R > 1.5$. Additionally, the azimuthal separation between the $\ell\ell\gamma$ system and the system formed by the two jets must be greater than 2.8. These jet variables are expected to have a different shape for the VBF signal and the background from QCD processes.

The $p_{T\ell}$ is defined as the component of the transverse momentum of the $\ell\ell\gamma$ system that is perpendicular to the difference of the three-momenta of the dilepton system and the photon candidate ($p_{T\ell} = |\vec{p}_T^{\ell\ell\gamma} \times \hat{t}|$, where $\hat{t} = (\vec{p}_T^{\ell\ell} - \vec{p}_T^\gamma)/|\vec{p}_T^{\ell\ell} - \vec{p}_T^\gamma|$). This quantity is strongly correlated with the transverse momentum of the $\ell\ell\gamma$ system, but has better experimental resolution [89,90]. Events failing the VBF-enriched selection, but having $p_{T\ell} > 100$ GeV, are assigned to the high- $p_{T\ell}$ category, which has a lower expected signal-to-background ratio than the VBF-enriched category, but is expected to have more events. The high- $p_{T\ell}$ category is expected to have an increased fraction of VBF and VH events as these production modes lead on average to higher Higgs boson p_T than ggF production.

The vast majority of selected events do not fall into the VBF-enriched or high- $p_{T\ell}$ categories discussed above, and are placed into the low- $p_{T\ell}$ category. The full list of all categories considered in the analysis, together with the expected yields for a 125.09 GeV Higgs boson decaying into $\ell\ell\gamma$, is shown in Table 1. The table also summarises the observed number of events in data in the $m_{\ell\ell\gamma}$ mass range of 110–160 GeV.

6. Signal and background modelling

To extract the observed signal yield, parametric functions are chosen to model the $\ell\ell\gamma$ invariant mass distributions of signal and background in each analysis category. A combined model is built from these functions and fit to the selected data in the $m_{\ell\ell\gamma}$ range of 110–160 GeV, simultaneously in all categories.

The signal model, including its parameters, is obtained by fitting a double-sided Crystal Ball function (DSCB) [91,92] to the $m_{\ell\ell\gamma}$ distribution obtained from the $H \rightarrow \gamma^*\gamma \rightarrow \ell\ell\gamma$ samples described in Section 3 after applying the event selection and categorisation from Section 5. The DSCB function features a Gaussian core and asymmetric power-law tails. A shift of +0.09 GeV is applied to the mean of the Gaussian function to account for the fact that the sample assumes a Higgs boson mass of 125 GeV. The effective signal mass resolution, defined as half the width containing 68% of the signal events, depends on the category and lies between 1.6 GeV (ee-merged high- p_T category) and 2.2 GeV (ee-resolved low- p_T category).

The $H \rightarrow \gamma\gamma$ process, which contributes as background to the electron categories through converted photons, is modelled using the same functions and parameters as the signal in the respective categories, and is normalised to the predicted SM yield. The parameterisations are compatible with the statistically limited distributions obtained from simulated $H \rightarrow \gamma\gamma$ events. This background contribution is relatively small (<2.5% and <7% of the expected $H \rightarrow \gamma^*\gamma \rightarrow \ell\ell\gamma$ signal in the ee-resolved channel and ee-merged channel, respectively) and is taken into account in the fitting procedure.

The non-resonant background is also estimated with parametric functions. The background normalisation and function parameters are allowed to float in the fit to data. The chosen functional forms are based on background templates that are built taking into account the contributions of different processes to the background. The function choice is performed separately for each category.

The dominant part of the background originates from the non-resonant $\ell\ell\gamma$ process. There is also a smaller background from events with misidentified photons, electrons, or muons. To estimate the fraction of events with a misidentified photon, a control region is formed using the signal selection, but dropping the photon isolation requirement and using it as a discriminating variable in a template fit. A background template enriched in events with misidentified photons is built by inverting the photon identification selection, with the prompt-photon contamination removed by subtracting its distribution found in simulated events. The template normalisation is obtained in the background-dominated sideband of the photon isolation distribution for each category separately. In the signal region, about 10% of all selected events have a misidentified photon, independently of the category. The fraction of events with a misidentified electron or muon that is in fact a hadronic jet, a lepton from heavy-flavour decays or an electron from a photon conversion, is estimated in a similar manner, using a control region in which the isolation selection is dropped for the softer lepton. The estimated fractions of events with misidentified leptons are 4% in the $\mu\mu$ low- $p_{T\ell}$ category, 2% in the ee-merged low- $p_{T\ell}$ category, and 30% in the ee-resolved low- $p_{T\ell}$ category. Events in the last category are separated into two groups depending on the angular distance between the electrons, as two populations with different misidentified-electron rates and mass distributions were found. The numbers in the other categories are extracted as well, but suffer from fairly large statistical uncertainties.

The invariant mass template for the non-resonant $\ell\ell\gamma$ background is built from the simulated events described in Section 3. The invariant mass templates for events with misidentified ob-

jects are obtained from background-dominated control regions, and scaled by the yields derived above. Reasonable agreement is observed between the templates containing the sum of all backgrounds and the sidebands of the $m_{\ell\ell\gamma}$ distributions in data (105–120 GeV and 130–160 GeV).

The choice of fit function for the non-resonant background is made in each category using signal-plus-background fits to the constructed background-only template by measuring the bias associated with each function, expressed as the number of fitted signal events, and choosing the function with the smallest number of degrees of freedom that satisfies the bias criteria described below.

The functional forms used to model the background are selected from the following: exponential ($e^{\alpha m_{\ell\ell\gamma}}$), exponential of a second-order polynomial ($e^{\alpha m_{\ell\ell\gamma} + \beta m_{\ell\ell\gamma}^2}$), and a power-law function ($m_{\ell\ell\gamma}^\alpha$), where α and β are free parameters. Signal hypotheses with m_H ranging from 121 GeV to 129 GeV are tested in steps of 1 GeV, and the fit bias is evaluated as the absolute maximum bias over this range (referred to as the ‘spurious signal’ in the following), similar to what is done in Ref. [1]. A function passes the test if the spurious signal is less than 10% of the expected number of $H \rightarrow \gamma^*\gamma \rightarrow \ell\ell\gamma$ events or less than 20% of the statistical uncertainty of the fitted spurious signal due to the expected number of background events. To account for statistical fluctuations in the background template, the criteria are relaxed by the statistical uncertainty due to the template [93]. Furthermore, in a background-only fit of the template in the mass range $110 < m_{\ell\ell\gamma} < 160$ GeV, the function must pass a χ^2 test with a probability larger than 1%. As described in Ref. [93], an additional check is performed by fitting both the chosen function and a function belonging to the same family with one more degree of freedom to the sidebands of the $m_{\ell\ell\gamma}$ distribution in data, to ensure the data do not prefer the more complex function. Following the procedure described above, the power-law function is selected for all categories, except for the $\mu\mu$ low- p_{T} and ee-merged low- p_{T} categories, which are best described by the second-order exponential polynomial, and the ee-resolved VBF-enriched category, for which the exponential function is chosen.

An unbinned extended likelihood function is formed from the product of each category’s parameterised signal-plus-background probability density function. Systematic uncertainties are considered in the form of nuisance parameters with Gaussian or log-normal constraints. They are correlated across all categories, except for the spurious-signal uncertainties. The latter are implemented for each category as a signal-like component with a yield parameter that is constrained by a Gaussian function, centred at zero, with a width corresponding to the estimated spurious signal. The Higgs boson mass is set to 125.09 ± 0.24 GeV [42].

The parameter of interest is the signal strength μ , which is defined as the ratio of the measured signal yield to the SM expectation, taking into account the uncertainties on the latter. The corresponding profile likelihood ratio is maximised to extract the best-fit μ [94]. A possible excess over the background-only hypothesis is quantified by a p -value using the profile likelihood ratio, evaluated for a vanishing $H \rightarrow \ell\ell\gamma$ branching ratio, as a test statistic. For all results, the asymptotic approximation is used [94]. Cross-checks of the best-fit μ and the p -value extracted with pseudo-experiments show good agreement with those obtained using the asymptotic approximation.

The measurement of the signal strength can be converted into a measurement of the Higgs boson production cross-section times the $H \rightarrow \ell\ell\gamma$ branching ratio in the fiducial region $m_{\ell\ell} < 30$ GeV. In this case, the included theory uncertainties are adjusted as discussed in Section 7, and the acceptance is extracted with the simulated samples described in Section 3.

7. Systematic uncertainties

The total observed systematic uncertainty in the signal strength measurement is 11%, which is about 35% of the size of the statistical uncertainty. Therefore, systematic uncertainties do not play a dominant role in this analysis.

The dominant experimental systematic uncertainties are due to the estimated biases in the fitted signal events (spurious signal, see Section 6). The corresponding uncertainty in the observed signal strength amounts to 6.1%. Other non-negligible systematic uncertainties relate to photon and lepton identification efficiencies in the simulated signal samples, in particular for merged-ee objects, as well as the energy/momenta calibration (see Section 4). Including jet uncertainties, which have a much smaller impact, these add up to 4.0%.

The uncertainty in the combined 2015–2018 integrated luminosity is 1.7% [95], obtained using the LUCID-2 detector [96] for the primary luminosity measurements. Uncertainties in the pile-up modelling contribute 1.7%. Uncertainties in the estimate of the $H \rightarrow \gamma\gamma$ background have a small impact of 0.7%. They include uncertainties in the photon-electron fake rate, and the uncertainties in the $\sigma(H) \times \mathcal{B}(H \rightarrow \gamma\gamma)$ measurement [93].

The assumed uncertainty in the $H \rightarrow \gamma^*\gamma \rightarrow \ell\ell\gamma$ branching ratio contributes 5.8%. The choice of QCD scales impacts the number and distribution of signal events in the different categories and is evaluated for the ggF, VBF, and VH production modes using a scheme similar to the one discussed in Ref. [93]. The corresponding uncertainty in the measured signal strength is 4.7%. Uncertainties in the PDF are evaluated using the eigenvectors of the PDF4LHC15 PDF set [33] and have a smaller effect of 2.3%. A conservative uncertainty of 50% is assigned to the normalisation of the $t\bar{t}H$, $gg \rightarrow ZH$, and bbH production modes, as no dedicated $H \rightarrow \gamma^*\gamma \rightarrow \ell\ell\gamma$ samples are available, with an impact of 0.8%. Parton shower uncertainties contribute only 0.3%.

For the $\sigma(H) \times \mathcal{B}(H \rightarrow \ell\ell\gamma)$ measurement, the effect of the theory uncertainties is reduced to 1.1% for the QCD scale and 0.9% for the PDF uncertainty, as only acceptance effects are considered, whereas the uncertainties in the predicted cross-sections and branching ratio are not applicable to this measurement.

8. Results

The $m_{\ell\ell\gamma}$ distributions of the selected events and the result of the global fit of the parametric signal-plus-background models to the data are shown in Fig. 3 for each event category.

The best-fit value of the signal-strength parameter is $\mu = 1.5 \pm 0.5 = 1.5 \pm 0.5$ (stat.) $^{+0.2}_{-0.1}$ (syst.), while the corresponding expected SM value is $\mu_{\text{exp}} = 1.0 \pm 0.5 = 1.0 \pm 0.5$ (stat.) $^{+0.2}_{-0.1}$ (syst.). The best-fit signal strength in the muon (electron) channel, obtained from a fit with two separate signal-strength parameters, is $\mu_{\mu\mu} = 1.9 \pm 0.7$ ($\mu_{ee} = 1.0 \pm 0.7$). Fig. 4 shows the results of the fit when the signal strength in each category is allowed to float independently. As anticipated in Table 1, the low- p_{T} categories, especially in the $\mu\mu$ channel, have the smallest uncertainties. It can be seen that all categories yield results that are consistent with each other and with the result of the single- μ fit.

For illustration, Fig. 5 shows the $m_{\ell\ell\gamma}$ distribution, with every data event reweighted by a category-dependent weight $\ln(1 + S_{90}/B_{90})$, where S_{90} is the number of signal events in the smallest window containing 90% of the expected signal and B_{90} is the expected number of background events in the same window, which consists of the resonant $H \rightarrow \gamma\gamma$ background as well as the non-resonant background. The latter is estimated from fits to the data sidebands using the background models.

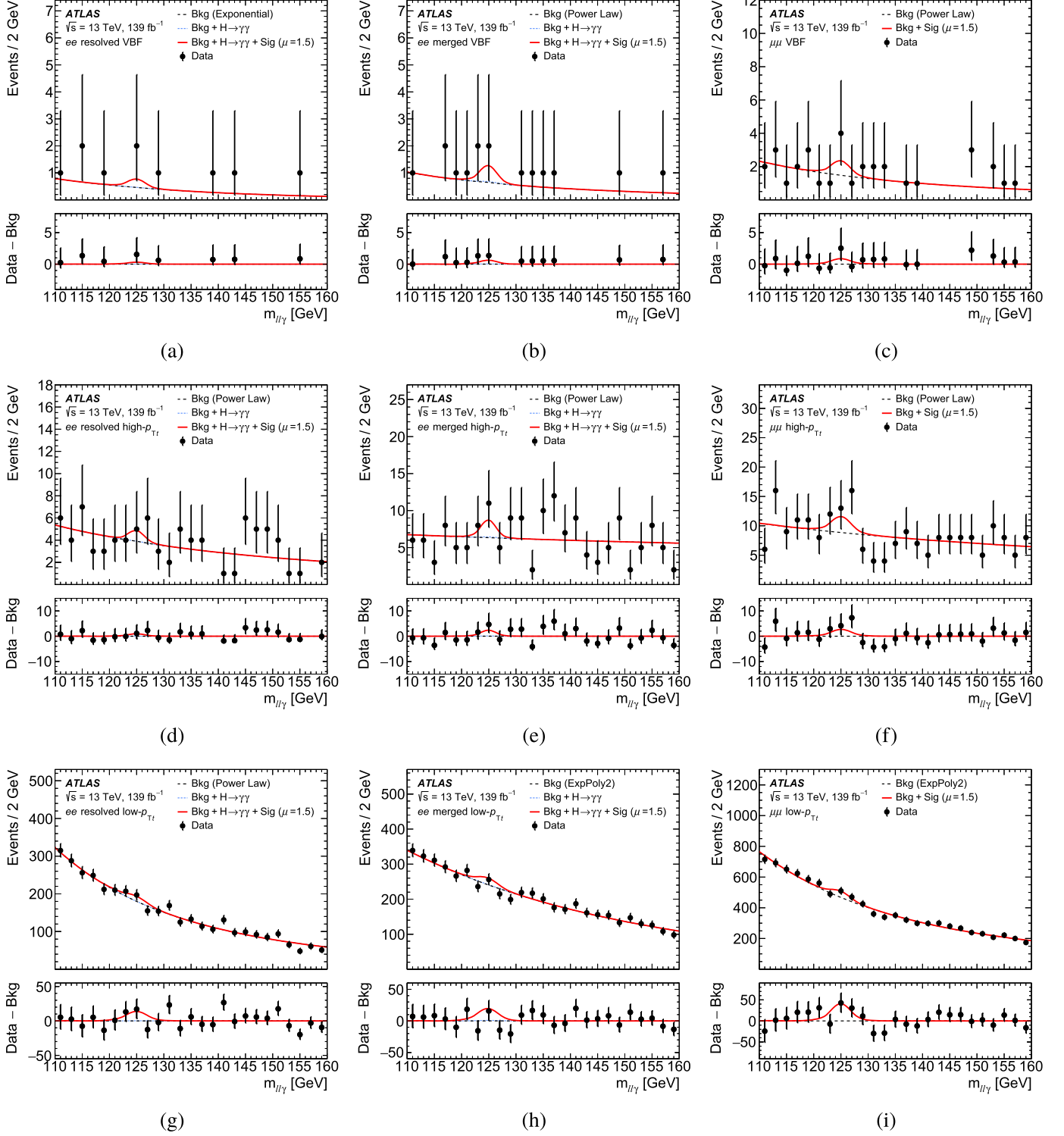


Fig. 3. $m_{ll\gamma}$ distributions of the selected events and the results of the global fit, for the VBF-enriched categories (a, b, c), the high- p_{Tt} categories (d, e, f), and the low- p_{Tt} categories (g, h, i). The ee -resolved categories are shown in the left column, the ee -merged categories in the middle and the $\mu\mu$ categories in the right column. The data are shown as the black circles with statistical uncertainties. The red curve shows the combined signal-plus-background model, the dashed black line shows the model of the non-resonant background component and the dotted blue line denotes the sum of the non-resonant background and the resonant $H \rightarrow \gamma\gamma$ background. The curves are obtained from the fit, i.e. they include the best-fit values of the parameter of interest and the nuisance parameters, including the spurious signal. The bottom panel shows the residuals of the data with respect to the non-resonant background component of the signal-plus-background fit.

The observed (expected) significance over the background-only hypothesis for a Higgs boson with a mass of 125.09 GeV is 3.2σ (2.1σ).

The Higgs boson production cross-section times the $H \rightarrow ll\gamma$ branching ratio for $m_{ll} < 30$ GeV is determined to be $8.7^{+2.8}_{-2.7}$ fb = 8.7 ± 2.7 (stat.) $^{+0.7}_{-0.6}$ (syst.) fb.

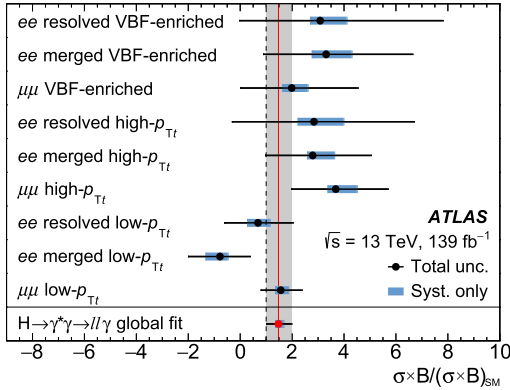


Fig. 4. Best-fit values of the signal-strength parameters for all event categories, in a fit where the signal strength in each category is allowed to float independently (black circles), compared with the result of the global fit (red circle and line) including its total uncertainty (grey band).

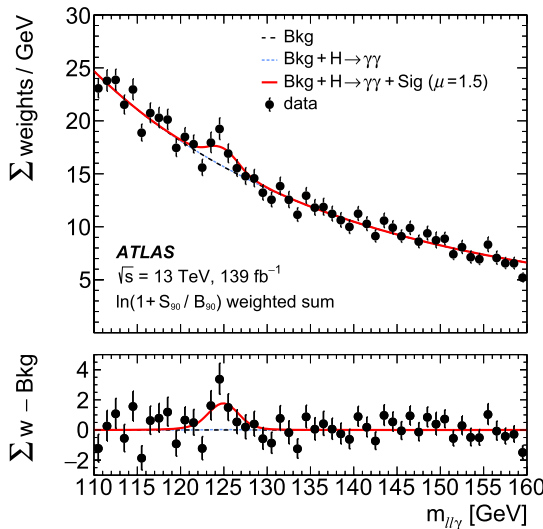


Fig. 5. $m_{ll\gamma}$ distribution, with every data event reweighted by a category-dependent weight, $\ln(1 + S_{90}/B_{90})$, where S_{90} is the number of signal events in the smallest window containing 90% of the expected signal, and B_{90} is the expected number of background events in the same window, estimated from fits to the data sidebands using the background models. The data are shown as the black circles with statistical uncertainties. The parameterised signal and backgrounds are also added up with the category-dependent weight. The red curve shows the combined signal-plus-background model when fitting all analysis categories simultaneously, the dashed black line shows the model of the non-resonant background component and the dotted blue line denotes the sum of the non-resonant background and the resonant $H \rightarrow \gamma\gamma$ background. The curves are obtained from the fit, i.e. they include the best-fit values of the parameter of interest and the nuisance parameters, including the spurious signal. The bottom panel shows the residuals of the data with respect to the non-resonant background component of the signal-plus-background fit.

9. Conclusion

A search for the Higgs boson decaying into a low-mass pair of electrons or muons and a photon is presented. The analysis is performed using a data set recorded by the ATLAS experiment at the LHC with proton–proton collisions at a centre-of-mass energy of 13 TeV, corresponding to an integrated luminosity of 139 fb^{-1} . For a Higgs boson with a mass of 125.09 GeV and $m_{ll} < 30 \text{ GeV}$, evidence for the $H \rightarrow ll\gamma$ process is found with a significance of 3.2σ over the background-only hypothesis, compared to an expected significance of 2.1σ . The best-fit value of the signal-strength parameter, defined as the ratio of the observed signal yield to the signal yield expected in the Standard Model, is $\mu = 1.5 \pm 0.5$. The Higgs boson production cross-section times the

$H \rightarrow ll\gamma$ branching ratio for $m_{ll} < 30 \text{ GeV}$ is determined to be $8.7^{+2.8}_{-2.7} \text{ fb}$. This result constitutes the first evidence for the decay of the Higgs boson into a pair of leptons and a photon, an important step towards probing Higgs boson couplings in this rare decay channel.

Declaration of competing interest

The authors declare that they have no known competing financial interests or personal relationships that could have appeared to influence the work reported in this paper.

Acknowledgements

We thank CERN for the very successful operation of the LHC, as well as the support staff from our institutions without whom ATLAS could not be operated efficiently.

We acknowledge the support of ANPCyT, Argentina; YerPhi, Armenia; ARC, Australia; BMWFW and FWF, Austria; ANAS, Azerbaijan; SSTC, Belarus; CNPq and FAPESP, Brazil; NSERC, NRC and CFI, Canada; CERN; ANID, Chile; CAS, MOST and NSFC, China; COLCIENCIAS, Colombia; MSMT CR, MPO CR and VSC CR, Czech Republic; DNRF and DNSRC, Denmark; IN2P3-CNRS and CEA-DRF/IRFU, France; SRNSFG, Georgia; BMBF, HGF and MPG, Germany; GSRT, Greece; RGC and Hong Kong SAR, China; ISF and Benoziyo Center, Israel; INFN, Italy; MEXT and JSPS, Japan; CNRST, Morocco; NWO, Netherlands; RCN, Norway; MNiSW and NCN, Poland; FCT, Portugal; MNE/IFA, Romania; JINR; MES of Russia and NRC KI, Russian Federation; MESTD, Serbia; MSSR, Slovakia; ARRS and MIZŠ, Slovenia; DST/NRF, South Africa; MICINN, Spain; SRC and Wallenberg Foundation, Sweden; SERI, SNSF and Cantons of Bern and Geneva, Switzerland; MOST, Taiwan; TAEK, Turkey; STFC, United Kingdom; DOE and NSF, United States of America. In addition, individual groups and members have received support from BCKDF, CANARIE, Compute Canada, CRC and IVADO, Canada; Beijing Municipal Science & Technology Commission, China; COST, ERC, ERDF, Horizon 2020 and Marie Skłodowska-Curie Actions, European Union; Investissements d’Avenir Labex, Investissements d’Avenir Idex and ANR, France; DFG and AvH Foundation, Germany; Herakleitos, Thales and Aristeia programmes co-financed by EU-ESF and the Greek NSRF, Greece; BSF-NSF and GIF, Israel; La Caixa Banking Foundation, CERCA Programme Generalitat de Catalunya and PROMETEO and GenT Programmes Generalitat Valenciana, Spain; Göran Gustafssons Stiftelser, Sweden; The Royal Society and Leverhulme Trust, United Kingdom.

The crucial computing support from all WLCG partners is acknowledged gratefully, in particular from CERN, the ATLAS Tier-1 facilities at TRIUMF (Canada), NDGF (Denmark, Norway, Sweden), CC-IN2P3 (France), KIT/GridKA (Germany), INFN-CNAF (Italy), NL-T1 (Netherlands), PIC (Spain), ASGC (Taiwan), RAL (UK) and BNL (USA), the Tier-2 facilities worldwide and large non-WLCG resource providers. Major contributors of computing resources are listed in Ref. [97].

References

- [1] ATLAS Collaboration, Observation of a new particle in the search for the Standard Model Higgs boson with the ATLAS detector at the LHC, Phys. Lett. B 716 (2012) 1, arXiv:1207.7214 [hep-ex].
- [2] CMS Collaboration, Observation of a new boson at a mass of 125 GeV with the CMS experiment at the LHC, Phys. Lett. B 716 (2012) 30, arXiv:1207.7235 [hep-ex].
- [3] ATLAS Collaboration, Study of the spin and parity of the Higgs boson in di-boson decays with the ATLAS detector, Eur. Phys. J. C 75 (2015) 476, arXiv: 1506.05669 [hep-ex]; Erratum: Eur. Phys. J. C 76 (2016) 152.
- [4] CMS Collaboration, Constraints on the spin-parity and anomalous HVV couplings of the Higgs boson in proton collisions at 7 and 8 TeV, Phys. Rev. D 92 (2015) 012004, arXiv:1411.3441 [hep-ex].

- [5] ATLAS CMS Collaborations, Measurements of the Higgs boson production and decay rates and constraints on its couplings from a combined ATLAS and CMS analysis of the LHC pp collision data at $\sqrt{s} = 7$ and 8 TeV, *J. High Energy Phys.* **08** (2016) 045, arXiv:1606.02266 [hep-ex].
- [6] CMS Collaboration, Combined measurements of Higgs boson couplings in proton-proton collisions at $\sqrt{s} = 13$ TeV, *Eur. Phys. J. C* **79** (2019) 421, arXiv:1809.10733 [hep-ex].
- [7] ATLAS Collaboration, Combined measurements of Higgs boson production and decay using up to 80 fb^{-1} of proton-proton collision data at $\sqrt{s} = 13$ TeV collected with the ATLAS experiment, *Phys. Rev. D* **101** (2020) 012002, arXiv:1909.02845 [hep-ex].
- [8] A. Kachanovich, U. Nierste, I. Nišandžić, Higgs boson decay into a lepton pair and a photon revisited, *Phys. Rev. D* **101** (2020) 073003, arXiv:2001.06516 [hep-ph].
- [9] A.Y. Korchin, V.A. Kovalchuk, Angular distribution and forward-backward asymmetry of the Higgs-boson decay to photon and lepton pair, *Eur. Phys. J. C* **74** (2014) 3141, arXiv:1408.0342 [hep-ph].
- [10] Y. Chen, A. Falkowski, I. Low, R. Vega-Morales, New observables for CP violation in Higgs decays, *Phys. Rev. D* **90** (2014) 113006, arXiv:1405.6723 [hep-ph].
- [11] L.-B. Chen, C.-F. Qiao, R.-L. Zhu, Reconstructing the 125 GeV SM Higgs boson through $\ell\ell\gamma$, *Phys. Lett. B* **726** (2013) 306, arXiv:1211.6058 [hep-ph]; Erratum: *Phys. Lett. B* **808** (2020) 135629.
- [12] G. Passarino, Higgs boson production and decay: Dalitz sector, *Phys. Lett. B* **727** (2013) 424, arXiv:1308.0422 [hep-ph].
- [13] CMS Collaboration, Search for the decay of a Higgs boson in the $\ell\ell\gamma$ channel in proton-proton collisions at $\sqrt{s} = 13$ TeV, *J. High Energy Phys.* **11** (2018) 152, arXiv:1806.05996 [hep-ex].
- [14] ATLAS Collaboration, A search for the $Z\gamma$ decay mode of the Higgs boson in pp collisions at $\sqrt{s} = 13$ TeV with the ATLAS detector, *Phys. Lett. B* **809** (2020) 135754, arXiv:2005.05382 [hep-ex].
- [15] CMS Collaboration, Search for a Higgs boson decaying into $\gamma^*\gamma \rightarrow \ell\ell\gamma$ with low dilepton mass in pp collisions at $\sqrt{s} = 8$ TeV, *Phys. Lett. B* **753** (2016) 341, arXiv:1507.03031 [hep-ex].
- [16] ATLAS Collaboration, The ATLAS experiment at the CERN Large Hadron Collider, *J. Instrum.* **3** (2008) S08003.
- [17] ATLAS Collaboration, ATLAS insertable B-layer technical design report, ATLAS-TDR-19, <https://cds.cern.ch/record/1291633>, 2010; ATLAS insertable B-layer technical design report addendum, ATLAS-TDR-19-ADD-1, <https://cds.cern.ch/record/1451888>, 2012.
- [18] B. Abbott, et al., Production and integration of the ATLAS insertable B-layer, *J. Instrum.* **13** (2018) T05008, arXiv:1803.00844 [physics.ins-det].
- [19] ATLAS Collaboration, Electron and photon performance measurements with the ATLAS detector using the 2015–2017 LHC proton-proton collision data, *J. Instrum.* **14** (2019) P12006, arXiv:1908.00005 [hep-ex].
- [20] ATLAS Collaboration, Performance of the ATLAS trigger system in 2015, *Eur. Phys. J. C* **77** (2017) 317, arXiv:1611.09661 [hep-ex].
- [21] ATLAS Collaboration, ATLAS data quality operations and performance for 2015–2018 data-taking, *J. Instrum.* **15** (2020) P04003, arXiv:1911.04632 [physics.ins-det].
- [22] ATLAS Collaboration, Performance of electron and photon triggers in ATLAS during LHC Run 2, *Eur. Phys. J. C* **80** (2020) 47, arXiv:1909.00761 [hep-ex].
- [23] ATLAS Collaboration, The ATLAS simulation infrastructure, *Eur. Phys. J. C* **70** (2010) 823, arXiv:1005.4568 [physics.ins-det].
- [24] S. Agostinelli, et al., GEANT4 - a simulation toolkit, *Nucl. Instrum. Methods A* **506** (2003) 250.
- [25] T. Sjöstrand, S. Mrenna, P. Skands, A brief introduction to PYTHIA 8.1, *Comput. Phys. Commun.* **178** (2008) 852, arXiv:0710.3820 [hep-ph].
- [26] R.D. Ball, et al., Parton distributions with LHC data, *Nucl. Phys. B* **867** (2013) 244, arXiv:1207.1303 [hep-ph].
- [27] ATLAS Collaboration, The Pythia 8 A3 tune description of ATLAS minimum bias and inelastic measurements incorporating the Donnachie–Landshoff diffractive model, ATL-PHYS-PUB-2016-017, <https://cds.cern.ch/record/2206965>, 2016.
- [28] P. Nason, C. Oleari, NLO Higgs boson production via vector-boson fusion matched with shower in POWHEG, *J. High Energy Phys.* **02** (2010) 037, arXiv:0911.5299 [hep-ph].
- [29] S. Alioli, P. Nason, C. Oleari, E. Re, A general framework for implementing NLO calculations in shower Monte Carlo programs: the POWHEG BOX, *J. High Energy Phys.* **06** (2010) (using ATLAS svn revisions r2856 for v1, r3080 for v2 ggF, r3052 for v2 VBF, and r3133 for v2 VH) arXiv:1002.2581 [hep-ph].
- [30] P. Nason, A new method for combining NLO QCD with shower Monte Carlo algorithms, *J. High Energy Phys.* **11** (2004) 040, arXiv:hep-ph/0409146.
- [31] S. Frixione, P. Nason, C. Oleari, Matching NLO QCD computations with Parton Shower simulations: the POWHEG method, *J. High Energy Phys.* **11** (2007) 070, arXiv:0709.2092 [hep-ph].
- [32] H.B. Hartanto, B. Jager, L. Reina, D. Wackerlo, Higgs boson production in association with top quarks in the POWHEG BOX, *Phys. Rev. D* **91** (2015) 094003, arXiv:1501.04498 [hep-ph].
- [33] J. Butterworth, et al., PDF4LHC recommendations for LHC Run II, *J. Phys. G* **43** (2016) 023001, arXiv:1510.03865 [hep-ph].
- [34] K. Hamilton, P. Nason, E. Re, G. Zanderighi, NNLOPS simulation of Higgs boson production, *J. High Energy Phys.* **10** (2013) 222, arXiv:1309.0017 [hep-ph].
- [35] K. Hamilton, P. Nason, G. Zanderighi, Finite quark-mass effects in the NNLOPS POWHEG+MinLO Higgs generator, *J. High Energy Phys.* **05** (2015) 140, arXiv:1501.04637 [hep-ph].
- [36] S. Catani, M. Grazzini, Next-to-Next-to-Leading-Order Subtraction Formalism in Hadron Collisions and its Application to Higgs-boson Production at the Large Hadron Collider, *Phys. Rev. Lett.* **98** (2007) 222002, arXiv:hep-ph/0703012 [hep-ph].
- [37] G. Cullen, et al., Automated one-loop calculations with GoSam, *Eur. Phys. J. C* **72** (2012) 1889, arXiv:1111.2034 [hep-ph].
- [38] K. Hamilton, P. Nason, C. Oleari, G. Zanderighi, Merging H/W/Z + 0 and 1 jet at NLO with no merging scale: a path to parton shower + NNLO matching, *J. High Energy Phys.* **05** (2013) 082, arXiv:1212.4504 [hep-ph].
- [39] G. Luisoni, P. Nason, C. Oleari, F. Tramontano, $HW^\pm/HZ + 0$ and 1 jet at NLO with the POWHEG BOX interfaced to GoSam and their merging within MINLO, *J. High Energy Phys.* **10** (2013) 083, arXiv:1306.2542 [hep-ph].
- [40] J. Bellm, et al., Herwig 7.0/Herwig++ 3.0 release note, *Eur. Phys. J. C* **76** (2016) 196, arXiv:1512.01178 [hep-ph].
- [41] D. de Florian, et al., Handbook of LHC Higgs cross sections: 4. Deciphering the nature of the Higgs sector, arXiv:1610.07922 [hep-ph], 2016.
- [42] ATLAS CMS Collaborations, Combined measurement of the Higgs boson mass in pp collisions at $\sqrt{s} = 7$ and 8 TeV with the ATLAS and CMS experiments, *Phys. Rev. Lett.* **114** (2015) 191803, arXiv:1503.07589 [hep-ex].
- [43] C. Anastasiou, C. Duhr, F. Dulat, F. Herzog, B. Mistlberger, Higgs boson gluon-fusion production in QCD at three loops, *Phys. Rev. Lett.* **114** (2015) 212001, arXiv:1503.06056 [hep-ph].
- [44] C. Anastasiou, et al., High precision determination of the gluon fusion Higgs boson cross-section at the LHC, *J. High Energy Phys.* **05** (2016) 058, arXiv:1602.00695 [hep-ph].
- [45] F. Dulat, A. Lazopoulos, B. Mistlberger, iHixs 2 – inclusive Higgs cross sections, *Comput. Phys. Commun.* **233** (2018) 243, arXiv:1802.00827 [hep-ph].
- [46] R.V. Harlander, K.J. Ozeren, Finite top mass effects for hadronic Higgs production at next-to-next-to-leading order, *J. High Energy Phys.* **11** (2009) 088, arXiv:0909.3420 [hep-ph].
- [47] R.V. Harlander, K.J. Ozeren, Top mass effects in Higgs production at next-to-next-to-leading order QCD: virtual corrections, *Phys. Lett. B* **679** (2009) 467, arXiv:0907.2997 [hep-ph].
- [48] R.V. Harlander, H. Mantler, S. Marzani, K.J. Ozeren, Higgs production in gluon fusion at next-to-next-to-leading order QCD for finite top mass, *Eur. Phys. J. C* **66** (2010) 359, arXiv:0912.2104 [hep-ph].
- [49] A. Pak, M. Rogal, M. Steinhauser, Finite top quark mass effects in NNLO Higgs boson production at LHC, *J. High Energy Phys.* **02** (2010) 025, arXiv:0911.4662 [hep-ph].
- [50] S. Actis, G. Passarino, C. Sturm, S. Uccirati, NLO electroweak corrections to Higgs boson production at hadron colliders, *Phys. Lett. B* **670** (2008) 12, arXiv:0809.1301 [hep-ph].
- [51] S. Actis, G. Passarino, C. Sturm, S. Uccirati, NNLO computational techniques: the cases $H \rightarrow \gamma\gamma$ and $H \rightarrow gg$, *Nucl. Phys. B* **811** (2009) 182, arXiv:0809.3667 [hep-ph].
- [52] C. Anastasiou, R. Boughezal, F. Petriello, Mixed QCD-electroweak corrections to Higgs boson production in gluon fusion, *J. High Energy Phys.* **04** (2009) 003, arXiv:0811.3458 [hep-ph].
- [53] U. Aglietti, R. Bonciani, G. Degrassi, A. Vicini, Two-loop light fermion contribution to Higgs production and decays, *Phys. Lett. B* **595** (2004) 432, arXiv:hep-ph/0404071 [hep-ph].
- [54] M. Bonetti, K. Melnikov, L. Tancredi, Higher order corrections to mixed QCD-EW contributions to Higgs boson production in gluon fusion, *Phys. Rev. D* **97** (2018) 056017; Erratum: *Phys. Rev. D* **97** (2018) 099906, arXiv:1801.10403 [hep-ph].
- [55] M. Ciccolini, A. Denner, S. Dittmaier, Strong and electroweak corrections to the production of a Higgs boson + 2 jets via weak interactions at the large hadron collider, *Phys. Rev. Lett.* **99** (2007) 161803, arXiv:0707.0381 [hep-ph].
- [56] M. Ciccolini, A. Denner, S. Dittmaier, Electroweak and QCD corrections to Higgs production via vector-boson fusion at the CERN LHC, *Phys. Rev. D* **77** (2008) 013002, arXiv:0710.4749 [hep-ph].
- [57] P. Bolzoni, F. Maltoni, S.-O. Moch, M. Zaro, Higgs boson production via vector-boson fusion at next-to-next-to-leading order in QCD, *Phys. Rev. Lett.* **105** (2010) 011801, arXiv:1003.4451 [hep-ph].
- [58] M.L. Ciccolini, S. Dittmaier, M. Krämer, Electroweak radiative corrections to associated WH and ZH production at hadron colliders, *Phys. Rev. D* **68** (2003) 073003, arXiv:hep-ph/0306234 [hep-ph].
- [59] O. Brein, A. Djouadi, R. Harlander, NNLO QCD corrections to the Higgs-strahlung processes at hadron colliders, *Phys. Lett. B* **579** (2004) 149, arXiv:hep-ph/0307206.
- [60] O. Brein, R. Harlander, M. Wiesemann, T. Zirke, Top-quark mediated effects in hadronic Higgs-Strahlung, *Eur. Phys. J. C* **72** (2012) 1868, arXiv:1111.0761 [hep-ph].
- [61] L. Altenkamp, S. Dittmaier, R.V. Harlander, H. Rzebak, T.J.E. Zirke, Gluon-induced Higgs-strahlung at next-to-leading order QCD, *J. High Energy Phys.* **02** (2013) 078, arXiv:1211.5015 [hep-ph].
- [62] A. Denner, S. Dittmaier, S. Kallweit, A. Mück, HAWK 2.0: a Monte Carlo program for Higgs production in vector-boson fusion and Higgs strahlung at hadron colliders, *Comput. Phys. Commun.* **195** (2015) 161, arXiv:1412.5390 [hep-ph].

- [63] O. Brein, R.V. Harlander, T.J.E. Zirke, [vh@nnlo](#) – Higgs Strahlung at hadron colliders, *Comput. Phys. Commun.* 184 (2013) 998, arXiv:1210.5347 [hep-ph].
- [64] R.V. Harlander, A. Kulesza, V. Theeuwes, T. Zirke, Soft gluon resummation for gluon-induced Higgs Strahlung, *J. High Energy Phys.* 11 (2014) 082, arXiv:1410.0217 [hep-ph].
- [65] R.V. Harlander, J. Klappert, S. Liebler, L. Simon, [vh@nnlo-v2](#): new physics in Higgs Strahlung, *J. High Energy Phys.* 05 (2018) 089, arXiv:1802.04817 [hep-ph].
- [66] W. Beenakker, et al., NLO QCD corrections to $t\bar{t}H$ production in hadron collisions, *Nucl. Phys. B* 653 (2003) 151, arXiv:hep-ph/0211352.
- [67] S. Dawson, C. Jackson, L.H. Orr, L. Reina, D. Wackerth, Associated Higgs boson production with top quarks at the CERN large hadron collider: NLO QCD corrections, *Phys. Rev. D* 68 (2003) 034022, arXiv:hep-ph/0305087.
- [68] Y. Zhang, W.-G. Ma, R.-Y. Zhang, C. Chen, L. Guo, QCD NLO and EW NLO corrections to $t\bar{t}H$ production with top quark decays at hadron collider, *Phys. Lett. B* 738 (2014) 1, arXiv:1407.1110 [hep-ph].
- [69] S. Frixione, V. Hirschi, D. Pagani, H.-S. Shao, M. Zaro, Electroweak and QCD corrections to top-pair hadroproduction in association with heavy bosons, *J. High Energy Phys.* 06 (2015) 184, arXiv:1504.03446 [hep-ph].
- [70] S. Dawson, C. Jackson, L. Reina, D. Wackerth, Exclusive Higgs boson production with bottom quarks at hadron colliders, *Phys. Rev. D* 69 (2004) 074027, arXiv:hep-ph/0311067.
- [71] S. Dittmaier, M. Krämer, M. Spira, Higgs radiation off bottom quarks at the Fermilab Tevatron and the CERN LHC, *Phys. Rev. D* 70 (2004) 074010, arXiv:hep-ph/0309204.
- [72] R. Harlander, M. Kramer, M. Schumacher, Bottom-quark associated Higgs-boson production: reconciling the four- and five-flavour scheme approach, arXiv:1112.3478 [hep-ph], 2011.
- [73] A. Abbasabadi, D. Bowser-Chao, D.A. Dicus, W.W. Repko, Radiative Higgs boson decays $H \rightarrow f\bar{f}\gamma$, *Phys. Rev. D* 55 (1997) 5647, arXiv:hep-ph/9611209.
- [74] A. Firan, R. Stroynowski, Internal conversions in Higgs decays to two photons, *Phys. Rev. D* 76 (2007) 057301, arXiv:0704.3987 [hep-ph].
- [75] D.A. Dicus, W.W. Repko, Calculation of the decay $H \rightarrow e\bar{e}\gamma$, *Phys. Rev. D* 87 (2013) 077301, arXiv:1302.2159 [hep-ph].
- [76] D.A. Dicus, W.W. Repko, Dalitz decay $H \rightarrow f\bar{f}\gamma$ as a background for $H \rightarrow \gamma\gamma$, *Phys. Rev. D* 89 (2014) 093013, arXiv:1402.5317 [hep-ph].
- [77] E. Bothmann, et al., Event generation with Sherpa 2.2, *SciPost Phys.* 7 (2019) 034, arXiv:1905.09127 [hep-ph].
- [78] R.D. Ball, et al., Parton distributions for the LHC Run II, *J. High Energy Phys.* 04 (2015) 040, arXiv:1410.8849 [hep-ph].
- [79] ATLAS Collaboration, Muon reconstruction performance of the ATLAS detector in proton-proton collision data at $\sqrt{s} = 13$ TeV, *Eur. Phys. J. C* 76 (2016) 292, arXiv:1603.05598 [hep-ex].
- [80] ATLAS Collaboration, Muon reconstruction and identification efficiency in ATLAS using the full Run 2 pp collision data set at $\sqrt{s} = 13$ TeV, arXiv:2012.00578 [hep-ex], 2020.
- [81] ATLAS Collaboration, Measurement of the photon identification efficiencies with the ATLAS detector using LHC Run 2 data collected in 2015 and 2016, *Eur. Phys. J. C* 79 (2019) 205, arXiv:1810.05087 [hep-ex].
- [82] ATLAS Collaboration, Electron reconstruction and identification in the ATLAS experiment using the 2015 and 2016 LHC proton-proton collision data at $\sqrt{s} = 13$ TeV, *Eur. Phys. J. C* 79 (2019) 639, arXiv:1902.04655 [hep-ex].
- [83] R. Frühwirth, Application of Kalman filtering to track and vertex fitting, *Nucl. Instrum. Methods A* 262 (1987) 444.
- [84] ATLAS Collaboration, Particle identification performance of the ATLAS transition radiation tracker, ATLAS-CONF-2011-128, <https://cds.cern.ch/record/1383793>, 2011.
- [85] ATLAS Collaboration, Topological cell clustering in the ATLAS calorimeters and its performance in LHC Run 1, *Eur. Phys. J. C* 77 (2017) 490, arXiv:1603.02934 [hep-ex].
- [86] M. Cacciari, G.P. Salam, G. Soyez, The anti- k_t jet clustering algorithm, *J. High Energy Phys.* 04 (2008) 063, arXiv:0802.1189 [hep-ph].
- [87] ATLAS Collaboration, Tagging and suppression of pileup jets with the ATLAS detector, ATLAS-CONF-2014-018, <https://cds.cern.ch/record/1700870>, 2014.
- [88] D.L. Rainwater, R. Szalapski, D. Zeppenfeld, Probing color singlet exchange in $Z + 2$ -jet events at the CERN LHC, *Phys. Rev. D* 54 (1996) 6680, arXiv:hep-ph/9605444.
- [89] OPAL Collaboration, Search for anomalous production of dilepton events with missing transverse momentum in e^+e^- collisions at $\sqrt{s} = 161$ GeV and 172 GeV, *Eur. Phys. J. C* 4 (1998) 47, arXiv:hep-ex/9710010.
- [90] M. Vesterinen, T. Wyatt, A novel technique for studying the Z boson transverse momentum distribution at hadron colliders, *Nucl. Instrum. Methods A* 602 (2009) 432, arXiv:0807.4956 [hep-ph].
- [91] M. Oreglia, A study of the reactions $\psi' \rightarrow \gamma\gamma\psi$, <https://www.slac.stanford.edu/cgi-wrap/getdoc/slac-r-236.pdf>, 1980.
- [92] ATLAS Collaboration, Search for scalar diphoton resonances in the mass range 65–600 GeV with the ATLAS detector in pp collision data at $\sqrt{s} = 8$ TeV, *Phys. Rev. Lett.* 113 (2014) 171801, arXiv:1407.6583 [hep-ex].
- [93] ATLAS Collaboration, Measurements of Higgs boson properties in the diphoton decay channel with 36 fb^{-1} of pp collision data at $\sqrt{s} = 13$ TeV with the ATLAS detector, *Phys. Rev. D* 98 (2018) 052005, arXiv:1802.04146 [hep-ex].
- [94] G. Cowan, K. Cranmer, E. Gross, O. Vitells, Asymptotic formulae for likelihood-based tests of new physics, *Eur. Phys. J. C* 71 (2011) 1554, arXiv:1007.1727 [physics.data-an]; Erratum: *Eur. Phys. J. C* 73 (2013) 2501.
- [95] ATLAS Collaboration, Luminosity determination in pp collisions at $\sqrt{s} = 13$ TeV using the ATLAS detector at the LHC, ATLAS-CONF-2019-021, <https://cds.cern.ch/record/2677054>, 2019.
- [96] G. Avoni, et al., The new LUCID-2 detector for luminosity measurement and monitoring in ATLAS, *J. Instrum.* 13 (2018) P07017.
- [97] ATLAS Collaboration, ATLAS computing acknowledgements, ATL-SOFT-PUB-2020-001, <https://cds.cern.ch/record/2717821>.

The ATLAS Collaboration

G. Aad ¹⁰¹, B. Abbott ¹²⁷, D.C. Abbott ¹⁰², A. Abed Abud ³⁶, K. Abeling ⁵³, D.K. Abhayasinghe ⁹³, S.H. Abidi ²⁹, O.S. AbouZeid ⁴⁰, N.L. Abraham ¹⁵⁵, H. Abramowicz ¹⁶⁰, H. Abreu ¹⁵⁹, Y. Abulaiti ⁶, A.C. Abusleme Hoffman ^{145a}, B.S. Acharya ^{66a,66b,p}, B. Achkar ⁵³, L. Adam ⁹⁹, C. Adam Bourdarios ⁵, L. Adamczyk ^{83a}, L. Adamek ¹⁶⁵, J. Adelman ¹²⁰, A. Adiguzel ^{12c,ad}, S. Adorni ⁵⁴, T. Adye ¹⁴², A.A. Affolder ¹⁴⁴, Y. Afik ¹⁵⁹, C. Agapopoulou ⁶⁴, M.N. Agaras ³⁸, A. Aggarwal ¹¹⁸, C. Agheorghiesei ^{27c}, J.A. Aguilar-Saavedra ^{138f,138a,ac}, A. Ahmad ³⁶, F. Ahmadov ⁷⁹, W.S. Ahmed ¹⁰³, X. Ai ⁴⁶, G. Aielli ^{73a,73b}, S. Akatsu ⁸⁵, M. Akbiyik ⁹⁹, T.P.A. Åkesson ⁹⁶, E. Akilli ⁵⁴, A.V. Akimov ¹¹⁰, K. Al Khoury ³⁹, G.L. Alberghi ^{23b,23a}, J. Albert ¹⁷⁴, M.J. Alconada Verzini ¹⁶⁰, S. Alderweireldt ³⁶, M. Aleksa ³⁶, I.N. Aleksandrov ⁷⁹, C. Alexa ^{27b}, T. Alexopoulos ¹⁰, A. Alfonsi ¹¹⁹, F. Alfonsi ^{23b,23a}, M. Alhroob ¹²⁷, B. Ali ¹⁴⁰, S. Ali ¹⁵⁷, M. Aliev ¹⁶⁴, G. Alimonti ^{68a}, C. Allaire ³⁶, B.M.M. Allbrooke ¹⁵⁵, P.P. Allport ²¹, A. Aloisio ^{69a,69b}, F. Alonso ⁸⁸, C. Alpigiani ¹⁴⁷, E. Alunno Camelia ^{73a,73b}, M. Alvarez Estevez ⁹⁸, M.G. Alviggi ^{69a,69b}, Y. Amaral Coutinho ^{80b}, A. Ambler ¹⁰³, L. Ambroz ¹³³, C. Amelung ³⁶, D. Amidei ¹⁰⁵, S.P. Amor Dos Santos ^{138a}, S. Amoroso ⁴⁶, C.S. Amrouche ⁵⁴, C. Anastopoulos ¹⁴⁸, N. Andari ¹⁴³, T. Andeen ¹¹, J.K. Anders ²⁰, S.Y. Andrean ^{45a,45b}, A. Andreazza ^{68a,68b}, V. Andrei ^{61a}, S. Angelidakis ⁹, A. Angerami ³⁹, A.V. Anisenkov ^{121b,121a}, A. Annovi ^{71a}, C. Antel ⁵⁴, M.T. Anthony ¹⁴⁸, E. Antipov ¹²⁸, M. Antonelli ⁵¹, D.J.A. Antrim ¹⁸, F. Anulli ^{72a}, M. Aoki ⁸¹, J.A. Aparisi Pozo ¹⁷², M.A. Aparo ¹⁵⁵, L. Aperio Bella ⁴⁶, N. Aranzabal ³⁶, V. Araujo Ferraz ^{80a}, C. Arcangeletti ⁵¹, A.T.H. Arce ⁴⁹, E. Arena ⁹⁰, J.-F. Arguin ¹⁰⁹, S. Argyropoulos ⁵², J.-H. Arling ⁴⁶, A.J. Armbruster ³⁶, A. Armstrong ¹⁶⁹, O. Arnaez ¹⁶⁵, H. Arnold ³⁶, Z.P. Arrubarrena Tame ¹¹³, G. Artoni ¹³³, H. Asada ¹¹⁶, K. Asai ¹²⁵, S. Asai ¹⁶², N.A. Asbah ⁵⁹, E.M. Asimakopoulou ¹⁷⁰, L. Asquith ¹⁵⁵, J. Assahsah ^{35e}, K. Assamagan ²⁹, R. Astalos ^{28a}, R.J. Atkin ^{33a},

- M. Atkinson 171, N.B. Atlay 19, H. Atmani 64, P.A. Atmasiddha 105, K. Augsten 140, V.A. Austrup 180,
 G. Avolio 36, M.K. Ayoub 15c, G. Azuelos 109,ak, D. Babal 28a, H. Bachacou 143, K. Bachas 161,
 F. Backman 45a,45b, P. Bagnaia 72a,72b, M. Bahmani 84, H. Bahrasemani 151, A.J. Bailey 172, V.R. Bailey 171,
 J.T. Baines 142, C. Bakalis 10, O.K. Baker 181, P.J. Bakker 119, E. Bakos 16, D. Bakshi Gupta 8, S. Balaji 156,
 R. Balasubramanian 119, E.M. Baldin 121b,121a, P. Balek 178, E. Ballabene 68a,68b, F. Balli 143, W.K. Balunas 133,
 J. Balz 99, E. Banas 84, M. Bandieramonte 137, A. Bandyopadhyay 19, L. Barak 160, W.M. Barbe 38,
 E.L. Barberio 104, D. Barberis 55b,55a, M. Barbero 101, G. Barbour 94, K.N. Barends 33a, T. Barillari 114,
 M-S. Barisits 36, J. Barkeloo 130, T. Barklow 152, B.M. Barnett 142, R.M. Barnett 18, Z. Barnovska-Blenessy 60a,
 A. Baroncelli 60a, G. Barone 29, A.J. Barr 133, L. Barranco Navarro 45a,45b, F. Barreiro 98,
 J. Barreiro Guimarães da Costa 15a, U. Barron 160, S. Barsov 136, F. Bartels 61a, R. Bartoldus 152,
 G. Bartolini 101, A.E. Barton 89, P. Bartos 28a, A. Basalaev 46, A. Basan 99, I. Bashta 74a,74b, A. Bassalat 64,ah,
 M.J. Basso 165, C.R. Basson 100, R.L. Bates 57, S. Batlamous 35f, J.R. Batley 32, B. Batool 150, M. Battaglia 144,
 M. Bauce 72a,72b, F. Bauer 143,* P. Bauer 24, H.S. Bawa 31, A. Bayirli 12c, J.B. Beacham 49, T. Beau 134,
 P.H. Beauchemin 168, F. Becherer 52, P. Bechtle 24, H.P. Beck 20,r, K. Becker 176, C. Becot 46, A.J. Beddall 12a,
 V.A. Bednyakov 79, C.P. Bee 154, T.A. Beermann 180, M. Begalli 80b, M. Begel 29, A. Behera 154, J.K. Behr 46,
 J.F. Beirer 53,36, F. Beisiegel 24, M. Belfkir 5, G. Bella 160, L. Bellagamba 23b, A. Bellerive 34, P. Bellos 21,
 K. Beloborodov 121b,121a, K. Belotskiy 111, N.L. Belyaev 111, D. Benchekroun 35a, Y. Benhammou 160,
 D.P. Benjamin 6, M. Benoit 29, J.R. Bensinger 26, S. Bentvelsen 119, L. Beresford 133, M. Beretta 51,
 D. Berge 19, E. Bergeaas Kuutmann 170, N. Berger 5, B. Bergmann 140, L.J. Bergsten 26, J. Beringer 18,
 S. Berlendis 7, G. Bernardi 134, C. Bernius 152, F.U. Bernlochner 24, T. Berry 93, P. Berta 46, A. Berthold 48,
 I.A. Bertram 89, O. Bessidskaia Bylund 180, S. Bethke 114, A. Betti 42, A.J. Bevan 92, S. Bhattacharya 154,
 D.S. Bhattacharya 175, P. Bhattacharai 26, V.S. Bhopatkar 6, R. Bi 137, R.M. Bianchi 137, O. Biebel 113, R. Bielski 36,
 K. Bierwagen 99, N.V. Biesuz 71a,71b, M. Biglietti 74a, T.R.V. Billoud 140, M. Bindi 53, A. Bingul 12d,
 C. Bini 72a,72b, S. Biondi 23b,23a, C.J. Birch-sykes 100, G.A. Bird 21,142, M. Birman 178, T. Bisanz 36,
 J.P. Biswal 3, D. Biswas 179,k, A. Bitadze 100, C. Bittrich 48, K. Bjørke 132, T. Blazek 28a, I. Bloch 46,
 C. Blocker 26, A. Blue 57, U. Blumenschein 92, G.J. Bobbink 119, V.S. Bobrovnikov 121b,121a, D. Bogavac 14,
 A.G. Bogdanchikov 121b,121a, C. Bohm 45a, V. Boisvert 93, P. Bokan 46, T. Bold 83a, M. Bomben 134,
 M. Bona 92, M. Boonekamp 143, C.D. Booth 93, A.G. Borbely 57, H.M. Borecka-Bielska 109, L.S. Borgna 94,
 G. Borissov 89, D. Bortoletto 133, D. Boscherini 23b, M. Bosman 14, J.D. Bossio Sola 103, K. Bouaouda 35a,
 J. Boudreau 137, E.V. Bouhova-Thacker 89, D. Boumediene 38, R. Bouquet 134, A. Boveia 126, J. Boyd 36,
 D. Boye 29, I.R. Boyko 79, A.J. Bozson 93, J. Bracinik 21, N. Brahimy 60d,60c, G. Brandt 180, O. Brandt 32,
 F. Braren 46, B. Brau 102, J.E. Brau 130, W.D. Breaden Madden 57, K. Brendlinger 46, R. Brener 159,
 L. Brenner 36, R. Brenner 170, S. Bressler 178, B. Brickwedde 99, D.L. Briglin 21, D. Britton 57, D. Britzger 114,
 I. Brock 24, R. Brock 106, G. Brooijmans 39, W.K. Brooks 145d, E. Brost 29, P.A. Bruckman de Renstrom 84,
 B. Brüers 46, D. Bruncko 28b, A. Bruni 23b, G. Bruni 23b, M. Bruschi 23b, N. Bruscino 72a,72b,
 L. Bryngemark 152, T. Buanes 17, Q. Buat 154, P. Buchholz 150, A.G. Buckley 57, I.A. Budagov 79,
 M.K. Bugge 132, O. Bulekov 111, B.A. Bullard 59, T.J. Burch 120, S. Burdin 90, C.D. Burgard 46, A.M. Burger 128,
 B. Burghgrave 8, J.T.P. Burr 46, C.D. Burton 11, J.C. Burzynski 102, V. Büscher 99, E. Buschmann 53,
 P.J. Bussey 57, J.M. Butler 25, C.M. Buttar 57, J.M. Butterworth 94, W. Buttlinger 142, C.J. Buxo Vazquez 106,
 A.R. Buzykaev 121b,121a, G. Cabras 23b,23a, S. Cabrera Urbán 172, D. Caforio 56, H. Cai 137, V.M.M. Cairo 152,
 O. Cakir 4a, N. Calace 36, P. Calafiura 18, G. Calderini 134, P. Calfayan 65, G. Callea 57, L.P. Caloba 80b,
 A. Caltabiano 73a,73b, S. Calvente Lopez 98, D. Calvet 38, S. Calvet 38, T.P. Calvet 101, M. Calvetti 71a,71b,
 R. Camacho Toro 134, S. Camarda 36, D. Camarero Munoz 98, P. Camarri 73a,73b, M.T. Camerlingo 74a,74b,
 D. Cameron 132, C. Camincher 36, M. Campanelli 94, A. Camplani 40, V. Canale 69a,69b, A. Canesse 103,
 M. Cano Bret 77, J. Cantero 128, Y. Cao 171, M. Capua 41b,41a, R. Cardarelli 73a, F. Cardillo 172,
 G. Carducci 41b,41a, T. Carli 36, G. Carlino 69a, B.T. Carlson 137, E.M. Carlson 174,166a, L. Carminati 68a,68b,
 M. Carnesale 72a,72b, R.M.D. Carney 152, S. Caron 118, E. Carquin 145d, S. Carrá 46, G. Carratta 23b,23a,
 J.W.S. Carter 165, T.M. Carter 50, D. Casadei 33c, M.P. Casado 14,h, A.F. Casha 165, E.G. Castiglio 181,
 F.L. Castillo 172, L. Castillo Garcia 14, V. Castillo Gimenez 172, N.F. Castro 138a,138e, A. Catinaccio 36,
 J.R. Catmore 132, A. Cattai 36, V. Cavalieri 29, N. Cavalli 23b,23a, V. Cavasinni 71a,71b, E. Celebi 12b, F. Celli 133,
 K. Cerny 129, A.S. Cerqueira 80a, A. Cerri 155, L. Cerrito 73a,73b, F. Cerutti 18, A. Cervelli 23b,23a, S.A. Cetin 12b,
 Z. Chadi 35a, D. Chakraborty 120, M. Chala 138f, J. Chan 179, W.S. Chan 119, W.Y. Chan 90, J.D. Chapman 32,
 B. Chargeishvili 158b, D.G. Charlton 21, T.P. Charman 92, M. Chatterjee 20, C.C. Chau 34, S. Chekanov 6,

- S.V. Chekulaev ^{166a}, G.A. Chelkov ^{79,af}, B. Chen ⁷⁸, C. Chen ^{60a}, C.H. Chen ⁷⁸, H. Chen ^{15c}, H. Chen ²⁹, J. Chen ^{60a}, J. Chen ³⁹, J. Chen ²⁶, S. Chen ¹³⁵, S.J. Chen ^{15c}, X. Chen ^{15b}, Y. Chen ^{60a}, Y.-H. Chen ⁴⁶, C.L. Cheng ¹⁷⁹, H.C. Cheng ^{62a}, H.J. Cheng ^{15a}, A. Cheplakov ⁷⁹, E. Cheremushkina ⁴⁶, R. Cherkaoui El Moursli ^{35f}, E. Cheu ⁷, K. Cheung ⁶³, L. Chevalier ¹⁴³, V. Chiarella ⁵¹, G. Chiarelli ^{71a}, G. Chiodini ^{67a}, A.S. Chisholm ²¹, A. Chitan ^{27b}, I. Chiu ¹⁶², Y.H. Chiu ¹⁷⁴, M.V. Chizhov ^{79,t}, K. Choi ¹¹, A.R. Chomont ^{72a,72b}, Y. Chou ¹⁰², Y.S. Chow ¹¹⁹, L.D. Christopher ^{33f}, M.C. Chu ^{62a}, X. Chu ^{15a,15d}, J. Chudoba ¹³⁹, J.J. Chwastowski ⁸⁴, D. Cieri ¹¹⁴, K.M. Ciesla ⁸⁴, V. Cindro ⁹¹, I.A. Cioară ^{27b}, A. Ciocio ¹⁸, F. Cirotto ^{69a,69b}, Z.H. Citron ^{178,l}, M. Citterio ^{68a}, D.A. Ciubotaru ^{27b}, B.M. Ciungu ¹⁶⁵, A. Clark ⁵⁴, P.J. Clark ⁵⁰, S.E. Clawson ¹⁰⁰, C. Clement ^{45a,45b}, L. Clissa ^{23b,23a}, Y. Coadou ¹⁰¹, M. Cobal ^{66a,66c}, A. Coccaro ^{55b}, J. Cochran ⁷⁸, R. Coelho Lopes De Sa ¹⁰², S. Coelli ^{68a}, H. Cohen ¹⁶⁰, A.E.C. Coimbra ³⁶, B. Cole ³⁹, J. Collot ⁵⁸, P. Conde Muiño ^{138a,138h}, S.H. Connell ^{33c}, I.A. Connelly ⁵⁷, E.I. Conroy ¹³³, F. Conventi ^{69a,al}, A.M. Cooper-Sarkar ¹³³, F. Cormier ¹⁷³, L.D. Corpe ⁹⁴, M. Corradi ^{72a,72b}, E.E. Corrigan ⁹⁶, F. Corriveau ^{103,aa}, M.J. Costa ¹⁷², F. Costanza ⁵, D. Costanzo ¹⁴⁸, B.M. Cote ¹²⁶, G. Cowan ⁹³, J.W. Cowley ³², J. Crane ¹⁰⁰, K. Cranmer ¹²⁴, R.A. Creager ¹³⁵, S. Crépé-Renaudin ⁵⁸, F. Crescioli ¹³⁴, M. Cristinziani ¹⁵⁰, M. Cristoforetti ^{75a,75b,b}, V. Croft ¹⁶⁸, G. Crosetti ^{41b,41a}, A. Cueto ⁵, T. Cuhadar Donszelmann ¹⁶⁹, H. Cui ^{15a,15d}, A.R. Cukierman ¹⁵², W.R. Cunningham ⁵⁷, S. Czekierda ⁸⁴, P. Czodrowski ³⁶, M.M. Czurylo ^{61b}, M.J. Da Cunha Sargedas De Sousa ^{60b}, J.V. Da Fonseca Pinto ^{80b}, C. Da Via ¹⁰⁰, W. Dabrowski ^{83a}, T. Dado ⁴⁷, S. Dahbi ^{33f}, T. Dai ¹⁰⁵, C. Dallapiccola ¹⁰², M. Dam ⁴⁰, G. D'amen ²⁹, V. D'Amico ^{74a,74b}, J. Damp ⁹⁹, J.R. Dandoy ¹³⁵, M.F. Daneri ³⁰, M. Danninger ¹⁵¹, V. Dao ³⁶, G. Darbo ^{55b}, A. Dattagupta ¹³⁰, S. D'Auria ^{68a,68b}, C. David ^{166b}, T. Davidek ¹⁴¹, D.R. Davis ⁴⁹, B.R. Davis-purcell ³⁴, I. Dawson ⁹², K. De ⁸, R. De Asmundis ^{69a}, M. De Beurs ¹¹⁹, S. De Castro ^{23b,23a}, N. De Groot ¹¹⁸, P. de Jong ¹¹⁹, H. De la Torre ¹⁰⁶, A. De Maria ^{15c}, D. De Pedis ^{72a}, A. De Salvo ^{72a}, U. De Sanctis ^{73a,73b}, M. De Santis ^{73a,73b}, A. De Santo ¹⁵⁵, J.B. De Vivie De Regie ⁵⁸, D.V. Dedovich ⁷⁹, J. Degens ¹¹⁹, A.M. Deiana ⁴², J. Del Peso ⁹⁸, Y. Delabat Diaz ⁴⁶, F. Deliot ¹⁴³, C.M. Delitzsch ⁷, M. Della Pietra ^{69a,69b}, D. Della Volpe ⁵⁴, A. Dell'Acqua ³⁶, L. Dell'Asta ^{73a,73b}, M. Delmastro ⁵, P.A. Delsart ⁵⁸, S. Demers ¹⁸¹, M. Demichev ⁷⁹, G. Demontigny ¹⁰⁹, S.P. Denisov ¹²², L. D'Eramo ¹²⁰, D. Derendarz ⁸⁴, J.E. Derkaoui ^{35e}, F. Derue ¹³⁴, P. Dervan ⁹⁰, K. Desch ²⁴, K. Dette ¹⁶⁵, C. Deutsch ²⁴, P.O. Deviveiros ³⁶, F.A. Di Bello ^{72a,72b}, A. Di Ciaccio ^{73a,73b}, L. Di Ciaccio ⁵, C. Di Donato ^{69a,69b}, A. Di Girolamo ³⁶, G. Di Gregorio ^{71a,71b}, A. Di Luca ^{75a,75b}, B. Di Micco ^{74a,74b}, R. Di Nardo ^{74a,74b}, C. Diaconu ¹⁰¹, F.A. Dias ¹¹⁹, T. Dias Do Vale ^{138a}, M.A. Diaz ^{145a}, F.G. Diaz Capriles ²⁴, J. Dickinson ¹⁸, M. Didenko ¹⁶⁴, E.B. Diehl ¹⁰⁵, J. Dietrich ¹⁹, S. Díez Cornell ⁴⁶, C. Diez Pardos ¹⁵⁰, A. Dimitrijevska ¹⁸, W. Ding ^{15b}, J. Dingfelder ²⁴, S.J. Dittmeier ^{61b}, F. Dittus ³⁶, F. Djama ¹⁰¹, T. Djobava ^{158b}, J.I. Djuvsland ¹⁷, M.A.B. Do Vale ¹⁴⁶, M. Dobre ^{27b}, D. Dodsworth ²⁶, C. Doglioni ⁹⁶, J. Dolejsi ¹⁴¹, Z. Dolezal ¹⁴¹, M. Donadelli ^{80c}, B. Dong ^{60c}, J. Donini ³⁸, A. D'onofrio ^{15c}, M. D'Onofrio ⁹⁰, J. Dopke ¹⁴², A. Doria ^{69a}, M.T. Dova ⁸⁸, A.T. Doyle ⁵⁷, E. Drechsler ¹⁵¹, E. Dreyer ¹⁵¹, T. Dreyer ⁵³, A.S. Drobac ¹⁶⁸, D. Du ^{60b}, T.A. du Pree ¹¹⁹, Y. Duan ^{60d}, F. Dubinin ¹¹⁰, M. Dubovsky ^{28a}, A. Dubreuil ⁵⁴, E. Duchovni ¹⁷⁸, G. Duckeck ¹¹³, O.A. Ducu ^{36,27b}, D. Duda ¹¹⁴, A. Dudarev ³⁶, A.C. Dudder ⁹⁹, M. D'uffizi ¹⁰⁰, L. Duflot ⁶⁴, M. Dührssen ³⁶, C. Dülsen ¹⁸⁰, M. Dumancic ¹⁷⁸, A.E. Dumitriu ^{27b}, M. Dunford ^{61a}, S. Dungs ⁴⁷, A. Duperrin ¹⁰¹, H. Duran Yildiz ^{4a}, M. Düren ⁵⁶, A. Durglishvili ^{158b}, B. Dutta ⁴⁶, D. Duvnjak ¹, G.I. Dyckes ¹³⁵, M. Dyndal ^{83a}, S. Dysch ¹⁰⁰, B.S. Dziedzic ⁸⁴, B. Eckerova ^{28a}, M.G. Eggleston ⁴⁹, E. Egidio Purcino De Souza ^{80b}, L.F. Ehrke ⁵⁴, T. Eifert ⁸, G. Eigen ¹⁷, K. Einsweiler ¹⁸, T. Ekelof ¹⁷⁰, H. El Jarrari ^{35f}, A. El Moussaoui ^{35a}, V. Ellajosyula ¹⁷⁰, M. Ellert ¹⁷⁰, F. Ellinghaus ¹⁸⁰, A.A. Elliot ⁹², N. Ellis ³⁶, J. Elmsheuser ²⁹, M. Elsing ³⁶, D. Emeliyanov ¹⁴², A. Emerman ³⁹, Y. Enari ¹⁶², J. Erdmann ⁴⁷, A. Ereditato ²⁰, P.A. Erland ⁸⁴, M. Errenst ¹⁸⁰, M. Escalier ⁶⁴, C. Escobar ¹⁷², O. Estrada Pastor ¹⁷², E. Etzion ¹⁶⁰, G. Evans ^{138a}, H. Evans ⁶⁵, M.O. Evans ¹⁵⁵, A. Ezhilov ¹³⁶, F. Fabbri ⁵⁷, L. Fabbri ^{23b,23a}, V. Fabiani ¹¹⁸, G. Facini ¹⁷⁶, R.M. Fakhrutdinov ¹²², S. Falciano ^{72a}, P.J. Falke ²⁴, S. Falke ³⁶, J. Faltova ¹⁴¹, Y. Fan ^{15a}, Y. Fang ^{15a}, Y. Fang ^{15a}, G. Fanourakis ⁴⁴, M. Fanti ^{68a,68b}, M. Faraj ^{60c}, A. Farbin ⁸, A. Farilla ^{74a}, E.M. Farina ^{70a,70b}, T. Farooque ¹⁰⁶, S.M. Farrington ⁵⁰, P. Farthouat ³⁶, F. Fassi ^{35f}, D. Fassouliotis ⁹, M. Faucci Giannelli ^{73a,73b}, W.J. Fawcett ³², L. Fayard ⁶⁴, O.L. Fedin ^{136,q}, A. Fehr ²⁰, M. Feickert ¹⁷¹, L. Feligioni ¹⁰¹, A. Fell ¹⁴⁸, C. Feng ^{60b}, M. Feng ⁴⁹, M.J. Fenton ¹⁶⁹, A.B. Fenyuk ¹²², S.W. Ferguson ⁴³, J. Ferrando ⁴⁶, A. Ferrari ¹⁷⁰, P. Ferrari ¹¹⁹, R. Ferrari ^{70a}, D. Ferrere ⁵⁴, C. Ferretti ¹⁰⁵, F. Fiedler ⁹⁹, A. Filipčič ⁹¹, F. Filthaut ¹¹⁸, K.D. Finelli ²⁵, M.C.N. Fiolhais ^{138a,138c,a}, L. Fiorini ¹⁷², F. Fischer ¹¹³, J. Fischer ⁹⁹, W.C. Fisher ¹⁰⁶, T. Fitschen ²¹, I. Fleck ¹⁵⁰, P. Fleischmann ¹⁰⁵, T. Flick ¹⁸⁰, B.M. Flierl ¹¹³, L. Flores ¹³⁵, L.R. Flores Castillo ^{62a}, F.M. Follega ^{75a,75b}, N. Fomin ¹⁷, J.H. Foo ¹⁶⁵,

- G.T. Forcolin ^{75a,75b}, B.C. Forland ⁶⁵, A. Formica ¹⁴³, F.A. Förster ¹⁴, A.C. Forti ¹⁰⁰, E. Fortin ¹⁰¹, M.G. Foti ¹³³, D. Fournier ⁶⁴, H. Fox ⁸⁹, P. Francavilla ^{71a,71b}, S. Francescato ^{72a,72b}, M. Franchini ^{23b,23a}, S. Franchino ^{61a}, D. Francis ³⁶, L. Franco ⁵, L. Franconi ²⁰, M. Franklin ⁵⁹, G. Frattari ^{72a,72b}, P.M. Freeman ²¹, B. Freund ¹⁰⁹, W.S. Freund ^{80b}, E.M. Freundlich ⁴⁷, D.C. Frizzell ¹²⁷, D. Froidevaux ³⁶, J.A. Frost ¹³³, Y. Fu ^{60a}, M. Fujimoto ¹²⁵, E. Fullana Torregrosa ¹⁷², T. Fusayasu ¹¹⁵, J. Fuster ¹⁷², A. Gabrielli ^{23b,23a}, A. Gabrielli ³⁶, P. Gadow ⁴⁶, G. Gagliardi ^{55b,55a}, L.G. Gagnon ¹⁸, G.E. Gallardo ¹³³, E.J. Gallas ¹³³, B.J. Gallop ¹⁴², R. Gamboa Goni ⁹², K.K. Gan ¹²⁶, S. Ganguly ¹⁷⁸, J. Gao ^{60a}, Y. Gao ⁵⁰, Y.S. Gao ^{31,n}, F.M. Garay Walls ^{145a}, C. García ¹⁷², J.E. García Navarro ¹⁷², J.A. García Pascual ^{15a}, M. Garcia-Sciveres ¹⁸, R.W. Gardner ³⁷, D. Garg ⁷⁷, S. Gargiulo ⁵², C.A. Garner ¹⁶⁵, V. Garonne ¹³², S.J. Gasiorowski ¹⁴⁷, P. Gaspar ^{80b}, G. Gaudio ^{70a}, P. Gauzzi ^{72a,72b}, I.L. Gavrilenko ¹¹⁰, A. Gavrilyuk ¹²³, C. Gay ¹⁷³, G. Gaycken ⁴⁶, E.N. Gazis ¹⁰, A.A. Geanta ^{27b}, C.M. Gee ¹⁴⁴, C.N.P. Gee ¹⁴², J. Geisen ⁹⁶, M. Geisen ⁹⁹, C. Gemme ^{55b}, M.H. Genest ⁵⁸, C. Geng ¹⁰⁵, S. Gentile ^{72a,72b}, S. George ⁹³, T. Geralis ⁴⁴, L.O. Gerlach ⁵³, P. Gessinger-Befurt ⁹⁹, G. Gessner ⁴⁷, M. Ghasemi Bostanabad ¹⁷⁴, M. Ghneimat ¹⁵⁰, A. Ghosh ¹⁶⁹, A. Ghosh ⁷⁷, B. Giacobbe ^{23b}, S. Giagu ^{72a,72b}, N. Giangiacomi ¹⁶⁵, P. Giannetti ^{71a}, A. Giannini ^{69a,69b}, S.M. Gibson ⁹³, M. Gignac ¹⁴⁴, D.T. Gil ^{83b}, B.J. Gilbert ³⁹, D. Gillberg ³⁴, G. Gilles ¹⁸⁰, N.E.K. Gillwald ⁴⁶, D.M. Gingrich ^{3,ak}, M.P. Giordani ^{66a,66c}, P.F. Giraud ¹⁴³, G. Giugliarelli ^{66a,66c}, D. Giugni ^{68a}, F. Giuli ^{73a,73b}, S. Gkaitatzis ¹⁶¹, I. Gkialas ^{9,i}, E.L. Gkougkousis ¹⁴, P. Gkountoumis ¹⁰, L.K. Gladilin ¹¹², C. Glasman ⁹⁸, G.R. Gledhill ¹³⁰, M. Glisic ¹³⁰, I. Gnesi ^{41b,d}, M. Goblirsch-Kolb ²⁶, D. Godin ¹⁰⁹, S. Goldfarb ¹⁰⁴, T. Golling ⁵⁴, D. Golubkov ¹²², A. Gomes ^{138a,138b}, R. Goncalves Gama ⁵³, R. Gonçalo ^{138a,138c}, G. Gonella ¹³⁰, L. Gonella ²¹, A. Gongadze ⁷⁹, F. Gonnella ²¹, J.L. Gonski ³⁹, S. González de la Hoz ¹⁷², S. Gonzalez Fernandez ¹⁴, R. Gonzalez Lopez ⁹⁰, C. Gonzalez Renteria ¹⁸, R. Gonzalez Suarez ¹⁷⁰, S. Gonzalez-Sevilla ⁵⁴, G.R. Gonzalvo Rodriguez ¹⁷², R.Y. González Andana ^{145a}, L. Goossens ³⁶, N.A. Gorasia ²¹, P.A. Gorbounov ¹²³, H.A. Gordon ²⁹, B. Gorini ³⁶, E. Gorini ^{67a,67b}, A. Gorišek ⁹¹, A.T. Goshaw ⁴⁹, M.I. Gostkin ⁷⁹, C.A. Gottardo ¹¹⁸, M. Gouighri ^{35b}, V. Goumarre ⁴⁶, A.G. Goussiou ¹⁴⁷, N. Govender ^{33c}, C. Goy ⁵, I. Grabowska-Bold ^{83a}, K. Graham ³⁴, E. Gramstad ¹³², S. Grancagnolo ¹⁹, M. Grandi ¹⁵⁵, V. Gratchev ¹³⁶, P.M. Gravila ^{27f}, F.G. Gravili ^{67a,67b}, H.M. Gray ¹⁸, C. Grefe ²⁴, I.M. Gregor ⁴⁶, P. Grenier ¹⁵², K. Grevtsov ⁴⁶, C. Grieco ¹⁴, N.A. Grieser ¹²⁷, A.A. Grillo ¹⁴⁴, K. Grimm ^{31,m}, S. Grinstein ^{14,x}, J.-F. Grivaz ⁶⁴, S. Groh ⁹⁹, E. Gross ¹⁷⁸, J. Grosse-Knetter ⁵³, Z.J. Grout ⁹⁴, C. Grud ¹⁰⁵, A. Grummer ¹¹⁷, J.C. Grundy ¹³³, L. Guan ¹⁰⁵, W. Guan ¹⁷⁹, C. Gubbels ¹⁷³, J. Guenther ³⁶, J.G.R. Guerrero Rojas ¹⁷², F. Guescini ¹¹⁴, D. Guest ¹⁹, R. Gugel ⁹⁹, A. Guida ⁴⁶, T. Guillemin ⁵, S. Guindon ³⁶, J. Guo ^{60c}, L. Guo ⁶⁴, Y. Guo ¹⁰⁵, R. Gupta ⁴⁶, S. Gurbuz ²⁴, G. Gustavino ¹²⁷, M. Guth ⁵², P. Gutierrez ¹²⁷, L.F. Gutierrez Zagazeta ¹³⁵, C. Gutschow ⁹⁴, C. Guyot ¹⁴³, C. Gwenlan ¹³³, C.B. Gwilliam ⁹⁰, E.S. Haaland ¹³², A. Haas ¹²⁴, M.H. Habedank ¹⁹, C. Haber ¹⁸, H.K. Hadavand ⁸, A. Hadef ⁹⁹, M. Haleem ¹⁷⁵, J. Haley ¹²⁸, J.J. Hall ¹⁴⁸, G. Halladjian ¹⁰⁶, G.D. Hallewell ¹⁰¹, L. Halser ²⁰, K. Hamano ¹⁷⁴, H. Hamdaoui ^{35f}, M. Hamer ²⁴, G.N. Hamity ⁵⁰, K. Han ^{60a}, L. Han ^{15c}, L. Han ^{60a}, S. Han ¹⁸, Y.F. Han ¹⁶⁵, K. Hanagaki ^{81,v}, M. Hance ¹⁴⁴, M.D. Hank ³⁷, R. Hankache ¹⁰⁰, E. Hansen ⁹⁶, J.B. Hansen ⁴⁰, J.D. Hansen ⁴⁰, M.C. Hansen ²⁴, P.H. Hansen ⁴⁰, E.C. Hanson ¹⁰⁰, K. Hara ¹⁶⁷, T. Harenberg ¹⁸⁰, S. Harkusha ¹⁰⁷, Y.T. Harris ¹³³, P.F. Harrison ¹⁷⁶, N.M. Hartman ¹⁵², N.M. Hartmann ¹¹³, Y. Hasegawa ¹⁴⁹, A. Hasib ⁵⁰, S. Hassani ¹⁴³, S. Haug ²⁰, R. Hauser ¹⁰⁶, M. Havranek ¹⁴⁰, C.M. Hawkes ²¹, R.J. Hawkings ³⁶, S. Hayashida ¹¹⁶, D. Hayden ¹⁰⁶, C. Hayes ¹⁰⁵, R.L. Hayes ¹⁷³, C.P. Hays ¹³³, J.M. Hays ⁹², H.S. Hayward ⁹⁰, S.J. Haywood ¹⁴², F. He ^{60a}, Y. He ¹⁶³, Y. He ¹³⁴, M.P. Heath ⁵⁰, V. Hedberg ⁹⁶, A.L. Heggelund ¹³², N.D. Hehir ⁹², C. Heidegger ⁵², K.K. Heidegger ⁵², W.D. Heidorn ⁷⁸, J. Heilman ³⁴, S. Heim ⁴⁶, T. Heim ¹⁸, B. Heinemann ^{46,ai}, J.G. Heinlein ¹³⁵, J.J. Heinrich ¹³⁰, L. Heinrich ³⁶, J. Hejbal ¹³⁹, L. Helary ⁴⁶, A. Held ¹²⁴, S. Hellesund ¹³², C.M. Helling ¹⁴⁴, S. Hellman ^{45a,45b}, C. Helsens ³⁶, R.C.W. Henderson ⁸⁹, L. Henkelmann ³², A.M. Henriques Correia ³⁶, H. Herde ¹⁵², Y. Hernández Jiménez ^{33f}, H. Herr ⁹⁹, M.G. Herrmann ¹¹³, T. Herrmann ⁴⁸, G. Herten ⁵², R. Hertenberger ¹¹³, L. Hervas ³⁶, N.P. Hessey ^{166a}, H. Hibi ⁸², S. Higashino ⁸¹, E. Higón-Rodriguez ¹⁷², K. Hildebrand ³⁷, K.K. Hill ²⁹, K.H. Hiller ⁴⁶, S.J. Hillier ²¹, M. Hils ⁴⁸, I. Hinchliffe ¹⁸, F. Hinterkeuser ²⁴, M. Hirose ¹³¹, S. Hirose ¹⁶⁷, D. Hirschbuehl ¹⁸⁰, B. Hiti ⁹¹, O. Hladik ¹³⁹, J. Hobbs ¹⁵⁴, R. Hobincu ^{27e}, N. Hod ¹⁷⁸, M.C. Hodgkinson ¹⁴⁸, B.H. Hodgkinson ³², A. Hoecker ³⁶, J. Hofer ⁴⁶, D. Hohn ⁵², T. Holm ²⁴, T.R. Holmes ³⁷, M. Holzbock ¹¹⁴, L.B.A.H. Hommels ³², B.P. Honan ¹⁰⁰, T.M. Hong ¹³⁷, J.C. Honig ⁵², A. Höngle ¹¹⁴, B.H. Hooberman ¹⁷¹, W.H. Hopkins ⁶, Y. Horii ¹¹⁶, P. Horn ⁴⁸, L.A. Horyn ³⁷, S. Hou ¹⁵⁷, J. Howarth ⁵⁷, J. Hoya ⁸⁸, M. Hrabovsky ¹²⁹, A. Hrynevich ¹⁰⁸, T. Hrynevich ⁵, P.J. Hsu ⁶³, S.-C. Hsu ¹⁴⁷, Q. Hu ³⁹, S. Hu ^{60c}, Y.F. Hu ^{15a,15d,am}, D.P. Huang ⁹⁴, X. Huang ^{15c},

- Y. Huang ^{60a}, Y. Huang ^{15a}, Z. Hubacek ¹⁴⁰, F. Hubaut ¹⁰¹, M. Huebner ²⁴, F. Huegging ²⁴, T.B. Huffman ¹³³,
 M. Huhtinen ³⁶, R. Hulskens ⁵⁸, R.F.H. Hunter ³⁴, N. Huseynov ^{79,ab}, J. Huston ¹⁰⁶, J. Huth ⁵⁹,
 R. Hyneman ¹⁵², S. Hyrych ^{28a}, G. Iacobucci ⁵⁴, G. Iakovidis ²⁹, I. Ibragimov ¹⁵⁰, L. Iconomidou-Fayard ⁶⁴,
 P. Iengo ³⁶, R. Ignazzi ⁴⁰, R. Iguchi ¹⁶², T. Iizawa ⁵⁴, Y. Ikegami ⁸¹, N. Illic ¹⁶⁵, H. Imam ^{35a}, G. Introzzi ^{70a,70b},
 M. Iodice ^{74a}, K. Iordanidou ^{166a}, V. Ippolito ^{72a,72b}, M. Ishino ¹⁶², W. Islam ¹²⁸, C. Issever ^{19,46}, S. Istin ^{12c},
 J.M. Iturbe Ponce ^{62a}, R. Iuppa ^{75a,75b}, A. Ivina ¹⁷⁸, J.M. Izen ⁴³, V. Izzo ^{69a}, P. Jacka ¹³⁹, P. Jackson ¹,
 R.M. Jacobs ⁴⁶, B.P. Jaeger ¹⁵¹, C.S. Jagfeld ¹¹³, G. Jäkel ¹⁸⁰, K.B. Jakobi ⁹⁹, K. Jakobs ⁵², T. Jakoubek ¹⁷⁸,
 J. Jamieson ⁵⁷, K.W. Janas ^{83a}, G. Jarlskog ⁹⁶, A.E. Jaspan ⁹⁰, N. Javadov ^{79,ab}, T. Javůrek ³⁶, M. Javurkova ¹⁰²,
 F. Jeanneau ¹⁴³, L. Jeanty ¹³⁰, J. Jejelava ^{158a}, P. Jenni ^{52,e}, S. Jézéquel ⁵, J. Jia ¹⁵⁴, Z. Jia ^{15c}, Y. Jiang ^{60a},
 S. Jiggins ⁵², F.A. Jimenez Morales ³⁸, J. Jimenez Pena ¹¹⁴, S. Jin ^{15c}, A. Jinaru ^{27b}, O. Jinnouchi ¹⁶³,
 H. Jivan ^{33f}, P. Johansson ¹⁴⁸, K.A. Johns ⁷, C.A. Johnson ⁶⁵, E. Jones ¹⁷⁶, R.W.L. Jones ⁸⁹, T.J. Jones ⁹⁰,
 J. Jovicevic ³⁶, X. Ju ¹⁸, J.J. Junggeburth ¹¹⁴, A. Juste Rozas ^{14,x}, A. Kaczmarska ⁸⁴, M. Kado ^{72a,72b},
 H. Kagan ¹²⁶, M. Kagan ¹⁵², A. Kahn ³⁹, C. Kahra ⁹⁹, T. Kaji ¹⁷⁷, E. Kajomovitz ¹⁵⁹, C.W. Kalderon ²⁹,
 A. Kaluza ⁹⁹, A. Kamenshchikov ¹²², M. Kaneda ¹⁶², N.J. Kang ¹⁴⁴, S. Kang ⁷⁸, Y. Kano ¹¹⁶, J. Kanzaki ⁸¹,
 D. Kar ^{33f}, K. Karava ¹³³, M.J. Kareem ^{166b}, I. Karkanias ¹⁶¹, S.N. Karpov ⁷⁹, Z.M. Karpova ⁷⁹,
 V. Kartvelishvili ⁸⁹, A.N. Karyukhin ¹²², E. Kasimi ¹⁶¹, C. Kato ^{60d}, J. Katzy ⁴⁶, K. Kawade ¹⁴⁹, K. Kawagoe ⁸⁷,
 T. Kawaguchi ¹¹⁶, T. Kawamoto ¹⁴³, G. Kawamura ⁵³, E.F. Kay ¹⁷⁴, F.I. Kaya ¹⁶⁸, S. Kazakos ¹⁴,
 V.F. Kazanin ^{121b,121a}, Y. Ke ¹⁵⁴, J.M. Keaveney ^{33a}, R. Keeler ¹⁷⁴, J.S. Keller ³⁴, D. Kelsey ¹⁵⁵, J.J. Kempster ²¹,
 J. Kendrick ²¹, K.E. Kennedy ³⁹, O. Kepka ¹³⁹, S. Kersten ¹⁸⁰, B.P. Kerševan ⁹¹, S. Ketabchi Haghighat ¹⁶⁵,
 F. Khalil-Zada ¹³, M. Khandoga ¹³⁴, A. Khanov ¹²⁸, A.G. Kharlamov ^{121b,121a}, T. Kharlamova ^{121b,121a},
 E.E. Khoda ¹⁷³, T.J. Khoo ¹⁹, G. Khoriauli ¹⁷⁵, E. Khramov ⁷⁹, J. Khubua ^{158b}, S. Kido ⁸², M. Kiehn ³⁶,
 A. Kilgallon ¹³⁰, E. Kim ¹⁶³, Y.K. Kim ³⁷, N. Kimura ⁹⁴, A. Kirchhoff ⁵³, D. Kirchmeier ⁴⁸, J. Kirk ¹⁴²,
 A.E. Kiryunin ¹¹⁴, T. Kishimoto ¹⁶², D.P. Kisliuk ¹⁶⁵, V. Kitali ⁴⁶, C. Kitsaki ¹⁰, O. Kivernyk ²⁴,
 T. Klapdor-Kleingrothaus ⁵², M. Klassen ^{61a}, C. Klein ³⁴, L. Klein ¹⁷⁵, M.H. Klein ¹⁰⁵, M. Klein ⁹⁰, U. Klein ⁹⁰,
 P. Klimek ³⁶, A. Klimentov ²⁹, F. Klimpel ³⁶, T. Klingl ²⁴, T. Klioutchnikova ³⁶, F.F. Klitzner ¹¹³, P. Kluit ¹¹⁹,
 S. Kluth ¹¹⁴, E. Kneringer ⁷⁶, T.M. Knight ¹⁶⁵, A. Knue ⁵², D. Kobayashi ⁸⁷, M. Kobel ⁴⁸, M. Kocian ¹⁵²,
 T. Kodama ¹⁶², P. Kodys ¹⁴¹, D.M. Koeck ¹⁵⁵, P.T. Koenig ²⁴, T. Koffas ³⁴, N.M. Köhler ³⁶, M. Kolb ¹⁴³,
 I. Koletsou ⁵, T. Komarek ¹²⁹, K. Köneke ⁵², A.X.Y. Kong ¹, T. Kono ¹²⁵, V. Konstantinides ⁹⁴,
 N. Konstantinidis ⁹⁴, B. Konya ⁹⁶, R. Kopeliansky ⁶⁵, S. Koperny ^{83a}, K. Korcyl ⁸⁴, K. Kordas ¹⁶¹, G. Koren ¹⁶⁰,
 A. Korn ⁹⁴, S. Korn ⁵³, I. Korolkov ¹⁴, E.V. Korolkova ¹⁴⁸, N. Korotkova ¹¹², O. Kortner ¹¹⁴, S. Kortner ¹¹⁴,
 V.V. Kostyukhin ^{148,164}, A. Kotsokechagia ⁶⁴, A. Kotwal ⁴⁹, A. Koulouris ⁹,
 A. Kourkoumeli-Charalampidi ^{70a,70b}, C. Kourkoumelis ⁹, E. Kourlitis ⁶, R. Kowalewski ¹⁷⁴,
 W. Kozanecki ¹⁴³, A.S. Kozhin ¹²², V.A. Kramarenko ¹¹², G. Kramberger ⁹¹, D. Krasnopevtsev ^{60a},
 M.W. Krasny ¹³⁴, A. Krasznahorkay ³⁶, J.A. Kremer ⁹⁹, J. Kretzschmar ⁹⁰, K. Kreul ¹⁹, P. Krieger ¹⁶⁵,
 F. Krieter ¹¹³, S. Krishnamurthy ¹⁰², A. Krishnan ^{61b}, M. Krivos ¹⁴¹, K. Krizka ¹⁸, K. Kroeninger ⁴⁷,
 H. Kroha ¹¹⁴, J. Kroll ¹³⁹, J. Kroll ¹³⁵, K.S. Krowpman ¹⁰⁶, U. Kruchonak ⁷⁹, H. Krüger ²⁴, N. Krumnack ⁷⁸,
 M.C. Kruse ⁴⁹, J.A. Krzysiak ⁸⁴, A. Kubota ¹⁶³, O. Kuchinskaia ¹⁶⁴, S. Kuday ^{4b}, D. Kuechler ⁴⁶,
 J.T. Kuechler ⁴⁶, S. Kuehn ³⁶, T. Kuhl ⁴⁶, V. Kukhtin ⁷⁹, Y. Kulchitsky ^{107,ae}, S. Kuleshov ^{145b}, M. Kumar ^{33f},
 N. Kumari ¹⁰¹, M. Kuna ⁵⁸, A. Kupco ¹³⁹, T. Kupfer ⁴⁷, O. Kuprash ⁵², H. Kurashige ⁸², L.L. Kurchaninov ^{166a},
 Y.A. Kurochkin ¹⁰⁷, A. Kurova ¹¹¹, M.G. Kurth ^{15a,15d}, E.S. Kuwertz ³⁶, M. Kuze ¹⁶³, A.K. Kvam ¹⁴⁷,
 J. Kvita ¹²⁹, T. Kwan ¹⁰³, C. Lacasta ¹⁷², F. Lacava ^{72a,72b}, D.P.J. Lack ¹⁰⁰, H. Lacker ¹⁹, D. Lacour ¹³⁴,
 E. Ladygin ⁷⁹, R. Lafaye ⁵, B. Laforge ¹³⁴, T. Lagouri ^{145c}, S. Lai ⁵³, I.K. Lakomiec ^{83a}, N. Lalloue ⁵⁸,
 J.E. Lambert ¹²⁷, S. Lammers ⁶⁵, W. Lampl ⁷, C. Lampoudis ¹⁶¹, E. Lançon ²⁹, U. Landgraf ⁵²,
 M.P.J. Landon ⁹², V.S. Lang ⁵², J.C. Lange ⁵³, R.J. Langenberg ¹⁰², A.J. Lankford ¹⁶⁹, F. Lanni ²⁹, K. Lantzsch ²⁴,
 A. Lanza ^{70a}, A. Lapertosa ^{55b,55a}, J.F. Laporte ¹⁴³, T. Lari ^{68a}, F. Lasagni Manghi ^{23b,23a}, M. Lassnig ³⁶,
 V. Latonova ¹³⁹, T.S. Lau ^{62a}, A. Laudrain ⁹⁹, A. Laurier ³⁴, M. Lavorgna ^{69a,69b}, S.D. Lawlor ⁹³,
 M. Lazzaroni ^{68a,68b}, B. Le ¹⁰⁰, A. Lebedev ⁷⁸, M. LeBlanc ⁷, T. LeCompte ⁶, F. Ledroit-Guillon ⁵⁸,
 A.C.A. Lee ⁹⁴, C.A. Lee ²⁹, G.R. Lee ¹⁷, L. Lee ⁵⁹, S.C. Lee ¹⁵⁷, S. Lee ⁷⁸, L.L. Leeuw ^{33c}, B. Lefebvre ^{166a},
 H.P. Lefebvre ⁹³, M. Lefebvre ¹⁷⁴, C. Leggett ¹⁸, K. Lehmann ¹⁵¹, N. Lehmann ²⁰, G. Lehmann Miotti ³⁶,
 W.A. Leight ⁴⁶, A. Leisos ^{161,w}, M.A.L. Leite ^{80c}, C.E. Leitgeb ¹¹³, R. Leitner ¹⁴¹, K.J.C. Leney ⁴², T. Lenz ²⁴,
 S. Leone ^{71a}, C. Leonidopoulos ⁵⁰, A. Leopold ¹³⁴, C. Leroy ¹⁰⁹, R. Les ¹⁰⁶, C.G. Lester ³², M. Levchenko ¹³⁶,
 J. Levêque ⁵, D. Levin ¹⁰⁵, L.J. Levinson ¹⁷⁸, D.J. Lewis ²¹, B. Li ^{15b}, B. Li ¹⁰⁵, C.-Q. Li ^{60c,60d}, F. Li ^{60c}, H. Li ^{60a},
 H. Li ^{60b}, J. Li ^{60c}, K. Li ¹⁴⁷, L. Li ^{60c}, M. Li ^{15a,15d}, Q.Y. Li ^{60a}, S. Li ^{60d,60c,c}, X. Li ⁴⁶, Y. Li ⁴⁶, Z. Li ^{60b}, Z. Li ¹³³

- Z. Li ¹⁰³, Z. Li ⁹⁰, Z. Liang ^{15a}, M. Liberatore ⁴⁶, B. Liberti ^{73a}, K. Lie ^{62c}, C.Y. Lin ³², K. Lin ¹⁰⁶, R.A. Linck ⁶⁵, R.E. Lindley ⁷, J.H. Lindon ²¹, A. Linss ⁴⁶, A.L. Lionti ⁵⁴, E. Lipeles ¹³⁵, A. Lipniacka ¹⁷, T.M. Liss ^{171,aj}, A. Lister ¹⁷³, J.D. Little ⁸, B. Liu ^{15a}, B.X. Liu ¹⁵¹, J.B. Liu ^{60a}, J.K.K. Liu ³⁷, K. Liu ^{60d,60c}, M. Liu ^{60a}, M.Y. Liu ^{60a}, P. Liu ^{15a}, X. Liu ^{60a}, Y. Liu ⁴⁶, Y. Liu ^{15a,15d}, Y.L. Liu ¹⁰⁵, Y.W. Liu ^{60a}, M. Livan ^{70a,70b}, A. Lleres ⁵⁸, J. Llorente Merino ¹⁵¹, S.L. Lloyd ⁹², E.M. Lobodzinska ⁴⁶, P. Loch ⁷, S. Loffredo ^{73a,73b}, T. Lohse ¹⁹, K. Lohwasser ¹⁴⁸, M. Lokajicek ¹³⁹, J.D. Long ¹⁷¹, R.E. Long ⁸⁹, I. Longarini ^{72a,72b}, L. Longo ³⁶, R. Longo ¹⁷¹, I. Lopez Paz ¹⁴, A. Lopez Solis ⁴⁶, J. Lorenz ¹¹³, N. Lorenzo Martinez ⁵, A.M. Lory ¹¹³, A. Lösle ⁵², X. Lou ^{45a,45b}, X. Lou ^{15a}, A. Lounis ⁶⁴, J. Love ⁶, P.A. Love ⁸⁹, J.J. Lozano Bahilo ¹⁷², G. Lu ^{15a}, M. Lu ^{60a}, S. Lu ¹³⁵, Y.J. Lu ⁶³, H.J. Lubatti ¹⁴⁷, C. Luci ^{72a,72b}, F.L. Lucio Alves ^{15c}, A. Lucotte ⁵⁸, F. Luehring ⁶⁵, I. Luise ¹⁵⁴, L. Luminari ^{72a}, B. Lund-Jensen ¹⁵³, N.A. Luongo ¹³⁰, M.S. Lutz ¹⁶⁰, D. Lynn ²⁹, H. Lyons ⁹⁰, R. Lysak ¹³⁹, E. Lytken ⁹⁶, F. Lyu ^{15a}, V. Lyubushkin ⁷⁹, T. Lyubushkina ⁷⁹, H. Ma ²⁹, LL. Ma ^{60b}, Y. Ma ⁹⁴, D.M. Mac Donell ¹⁷⁴, G. Maccarrone ⁵¹, C.M. Macdonald ¹⁴⁸, J.C. MacDonald ¹⁴⁸, R. Madar ³⁸, W.F. Mader ⁴⁸, M. Madugoda Ralalage Don ¹²⁸, N. Madysa ⁴⁸, J. Maeda ⁸², T. Maeno ²⁹, M. Maerker ⁴⁸, V. Magerl ⁵², J. Magro ^{66a,66c}, D.J. Mahon ³⁹, C. Maidantchik ^{80b}, A. Maio ^{138a,138b,138d}, K. Maj ^{83a}, O. Majersky ^{28a}, S. Majewski ¹³⁰, N. Makovec ⁶⁴, B. Malaescu ¹³⁴, Pa. Malecki ⁸⁴, V.P. Maleev ¹³⁶, F. Malek ⁵⁸, D. Malito ^{41b,41a}, U. Mallik ⁷⁷, C. Malone ³², S. Maltezos ¹⁰, S. Malyukov ⁷⁹, J. Mamuzic ¹⁷², G. Mancini ⁵¹, J.P. Mandalia ⁹², I. Mandić ⁹¹, L. Manhaes de Andrade Filho ^{80a}, I.M. Maniatis ¹⁶¹, M. Manisha ¹⁴³, J. Manjarres Ramos ⁴⁸, K.H. Mankinen ⁹⁶, A. Mann ¹¹³, A. Manousos ⁷⁶, B. Mansoulie ¹⁴³, I. Manthos ¹⁶¹, S. Manzoni ¹¹⁹, A. Marantis ¹⁶¹, L. Marchese ¹³³, G. Marchiori ¹³⁴, M. Marcisovsky ¹³⁹, L. Marcoccia ^{73a,73b}, C. Marcon ⁹⁶, M. Marjanovic ¹²⁷, Z. Marshall ¹⁸, S. Marti-Garcia ¹⁷², T.A. Martin ¹⁷⁶, V.J. Martin ⁵⁰, B. Martin dit Latour ¹⁷, L. Martinelli ^{74a,74b}, M. Martinez ^{14,x}, P. Martinez Agullo ¹⁷², V.I. Martinez Outschoorn ¹⁰², S. Martin-Haugh ¹⁴², V.S. Martoiu ^{27b}, A.C. Martyniuk ⁹⁴, A. Marzin ³⁶, S.R. Maschek ¹¹⁴, L. Masetti ⁹⁹, T. Mashimo ¹⁶², R. Mashinistov ¹¹⁰, J. Masik ¹⁰⁰, A.L. Maslennikov ^{121b,121a}, L. Massa ^{23b,23a}, P. Massarotti ^{69a,69b}, P. Mastrandrea ^{71a,71b}, A. Mastroberardino ^{41b,41a}, T. Masubuchi ¹⁶², D. Matakias ²⁹, T. Mathisen ¹⁷⁰, A. Matic ¹¹³, N. Matsuzawa ¹⁶², J. Maurer ^{27b}, B. Maček ⁹¹, D.A. Maximov ^{121b,121a}, R. Mazini ¹⁵⁷, I. Maznas ¹⁶¹, S.M. Mazza ¹⁴⁴, C. Mc Ginn ²⁹, J.P. Mc Gowan ¹⁰³, S.P. Mc Kee ¹⁰⁵, T.G. McCarthy ¹¹⁴, W.P. McCormack ¹⁸, E.F. McDonald ¹⁰⁴, A.E. McDougall ¹¹⁹, J.A. McFayden ¹⁵⁵, G. Mchedlidze ^{158b}, M.A. McKay ⁴², K.D. McLean ¹⁷⁴, S.J. McMahon ¹⁴², P.C. McNamara ¹⁰⁴, R.A. McPherson ^{174,aa}, J.E. Mdhluli ^{33f}, Z.A. Meadows ¹⁰², S. Meehan ³⁶, T. Megy ³⁸, S. Mehlhase ¹¹³, A. Mehta ⁹⁰, B. Meirose ⁴³, D. Melini ¹⁵⁹, B.R. Mellado Garcia ^{33f}, F. Meloni ⁴⁶, A. Melzer ²⁴, E.D. Mendes Gouveia ^{138a,138e}, A.M. Mendes Jacques Da Costa ²¹, H.Y. Meng ¹⁶⁵, L. Meng ³⁶, S. Menke ¹¹⁴, E. Meoni ^{41b,41a}, S.A.M. Merkt ¹³⁷, C. Merlassino ¹³³, P. Mermod ⁵⁴, L. Merola ^{69a,69b}, C. Meroni ^{68a}, G. Merz ¹⁰⁵, O. Meshkov ^{112,110}, J.K.R. Meshreki ¹⁵⁰, J. Metcalfe ⁶, A.S. Mete ⁶, C. Meyer ⁶⁵, J-P. Meyer ¹⁴³, M. Michetti ¹⁹, R.P. Middleton ¹⁴², L. Mijović ⁵⁰, G. Mikenberg ¹⁷⁸, M. Mikestikova ¹³⁹, M. Mikuž ⁹¹, H. Mildner ¹⁴⁸, A. Milic ¹⁶⁵, C.D. Milke ⁴², D.W. Miller ³⁷, L.S. Miller ³⁴, A. Milov ¹⁷⁸, D.A. Milstead ^{45a,45b}, A.A. Minaenko ¹²², I.A. Minashvili ^{158b}, L. Mince ⁵⁷, A.I. Mincer ¹²⁴, B. Mindur ^{83a}, M. Mineev ⁷⁹, Y. Minegishi ¹⁶², Y. Mino ⁸⁵, L.M. Mir ¹⁴, M. Miralles Lopez ¹⁷², M. Mironova ¹³³, T. Mitani ¹⁷⁷, V.A. Mitsou ¹⁷², M. Mittal ^{60c}, O. Miu ¹⁶⁵, P.S. Miyagawa ⁹², Y. Miyazaki ⁸⁷, A. Mizukami ⁸¹, J.U. Mjörnmark ⁹⁶, T. Mkrtchyan ^{61a}, M. Mlynarikova ¹²⁰, T. Moa ^{45a,45b}, S. Mobius ⁵³, K. Mochizuki ¹⁰⁹, P. Moder ⁴⁶, P. Mogg ¹¹³, S. Mohapatra ³⁹, G. Mokgatitswane ^{33f}, B. Mondal ¹⁵⁰, S. Mondal ¹⁴⁰, K. Mönig ⁴⁶, E. Monnier ¹⁰¹, A. Montalbano ¹⁵¹, J. Montejo Berlingen ³⁶, M. Montella ⁹⁴, F. Monticelli ⁸⁸, N. Morange ⁶⁴, A.L. Moreira De Carvalho ^{138a}, M. Moreno Llácer ¹⁷², C. Moreno Martinez ¹⁴, P. Morettini ^{55b}, M. Morgenstern ¹⁵⁹, S. Morgenstern ¹⁷⁶, D. Mori ¹⁵¹, M. Morii ⁵⁹, M. Morinaga ¹⁷⁷, V. Morisbak ¹³², A.K. Morley ³⁶, A.P. Morris ⁹⁴, L. Morvaj ³⁶, P. Moschovakos ³⁶, B. Moser ¹¹⁹, M. Mosidze ^{158b}, T. Moskalets ⁵², P. Moskvitina ¹¹⁸, J. Moss ^{31,o}, E.J.W. Moyse ¹⁰², S. Muanza ¹⁰¹, J. Mueller ¹³⁷, D. Muenstermann ⁸⁹, G.A. Mullier ⁹⁶, J.J. Mullin ¹³⁵, D.P. Mungo ^{68a,68b}, J.L. Munoz Martinez ¹⁴, F.J. Munoz Sanchez ¹⁰⁰, M. Murin ¹⁰⁰, P. Murin ^{28b}, W.J. Murray ^{176,142}, A. Murrone ^{68a,68b}, J.M. Muse ¹²⁷, M. Muškinja ¹⁸, C. Mwewa ²⁹, A.G. Myagkov ^{122,af}, A.A. Myers ¹³⁷, G. Myers ⁶⁵, J. Myers ¹³⁰, M. Myska ¹⁴⁰, B.P. Nachman ¹⁸, O. Nackenhorst ⁴⁷, A. Nag Nag ⁴⁸, K. Nagai ¹³³, K. Nagano ⁸¹, J.L. Nagle ²⁹, E. Nagy ¹⁰¹, A.M. Nairz ³⁶, Y. Nakahama ¹¹⁶, K. Nakamura ⁸¹, H. Nanjo ¹³¹, F. Napolitano ^{61a}, R.F. Naranjo Garcia ⁴⁶, R. Narayan ⁴², I. Naryshkin ¹³⁶, M. Naseri ³⁴, T. Naumann ⁴⁶, G. Navarro ^{22a}, J. Navarro-Gonzalez ¹⁷², P.Y. Nechaeva ¹¹⁰, F. Nechansky ⁴⁶, T.J. Neep ²¹, A. Negri ^{70a,70b}, M. Negrini ^{23b}, C. Nellist ¹¹⁸, C. Nelson ¹⁰³, K. Nelson ¹⁰⁵, M.E. Nelson ^{45a,45b}, S. Nemecek ¹³⁹, M. Nessi ^{36,g}, M.S. Neubauer ¹⁷¹, F. Neuhaus ⁹⁹,

- M. Neumann 180, R. Newhouse 173, P.R. Newman 21, C.W. Ng 137, Y.S. Ng 19, Y.W.Y. Ng 169, B. Ngair 35f,
 H.D.N. Nguyen 101, T. Nguyen Manh 109, E. Nibigira 38, R.B. Nickerson 133, R. Nicolaïdou 143, D.S. Nielsen 40,
 J. Nielsen 144, M. Niemeyer 53, N. Nikiforou 11, V. Nikolaenko 122,af, I. Nikolic-Audit 134, K. Nikolopoulos 21,
 P. Nilsson 29, H.R. Nindhito 54, A. Nisati 72a, N. Nishu 3, R. Nisius 114, T. Nitta 177, T. Nobe 162, D.L. Noel 32,
 Y. Noguchi 85, I. Nomidis 134, M.A. Nomura 29, M.B. Norfolk 148, R.R.B. Norisam 94, J. Novak 91, T. Novak 46,
 O. Novgorodova 48, L. Novotny 140, R. Novotny 117, L. Nozka 129, K. Ntekas 169, E. Nurse 94,
 F.G. Oakham 34,ak, J. Ocariz 134, A. Ochi 82, I. Ochoa 138a, J.P. Ochoa-Ricoux 145a, K. O'Connor 26, S. Oda 87,
 S. Odaka 81, S. Oerdekk 53, A. Ogrodnik 83a, A. Oh 100, C.C. Ohm 153, H. Oide 163, R. Oishi 162, M.L. Ojeda 165,
 Y. Okazaki 85, M.W. O'Keefe 90, Y. Okumura 162, A. Olariu 27b, L.F. Oleiro Seabra 138a, S.A. Olivares Pino 145c,
 D. Oliveira Damazio 29, D. Oliveira Goncalves 80a, J.L. Oliver 1, M.J.R. Olsson 169, A. Olszewski 84,
 J. Olszowska 84, Ö.O. Öncel 24, D.C. O'Neil 151, A.P. O'Neill 133, A. Onofre 138a,138e, P.U.E. Onyisi 11,
 H. Oppen 132, R.G. Oreamuno Madriz 120, M.J. Oreglia 37, G.E. Orellana 88, D. Orestano 74a,74b,
 N. Orlando 14, R.S. Orr 165, V. O'Shea 57, R. Ospanov 60a, G. Otero y Garzon 30, H. Otono 87, P.S. Ott 61a,
 G.J. Ottino 18, M. Ouchrif 35e, J. Ouellette 29, F. Ould-Saada 132, A. Ouraou 143,* Q. Ouyang 15a, M. Owen 57,
 R.E. Owen 142, V.E. Ozcan 12c, N. Ozturk 8, J. Pacalt 129, H.A. Pacey 32, K. Pachal 49, A. Pacheco Pages 14,
 C. Padilla Aranda 14, S. Pagan Griso 18, G. Palacino 65, S. Palazzo 50, S. Palestini 36, M. Palka 83b, P. Palni 83a,
 D.K. Panchal 11, C.E. Pandini 54, J.G. Panduro Vazquez 93, P. Pani 46, G. Panizzo 66a,66c, L. Paolozzi 54,
 C. Papadatos 109, S. Parajuli 42, A. Paramonov 6, C. Paraskevopoulos 10, D. Paredes Hernandez 62b,
 S.R. Paredes Saenz 133, B. Parida 178, T.H. Park 165, A.J. Parker 31, M.A. Parker 32, F. Parodi 55b,55a,
 E.W. Parrish 120, J.A. Parsons 39, U. Parzefall 52, L. Pascual Dominguez 134, V.R. Pascuzzi 18,
 J.M.P. Pasner 144, F. Pasquali 119, E. Pasqualucci 72a, S. Passaggio 55b, F. Pastore 93, P. Pasuwan 45a,45b,
 J.R. Pater 100, A. Pathak 179,k, J. Patton 90, T. Pauly 36, J. Pearkes 152, M. Pedersen 132, L. Pedraza Diaz 118,
 R. Pedro 138a, T. Peiffer 53, S.V. Peleganchuk 121b,121a, O. Penc 139, C. Peng 62b, H. Peng 60a, M. Penzin 164,
 B.S. Peralva 80a, M.M. Perego 64, A.P. Pereira Peixoto 138a, L. Pereira Sanchez 45a,45b, D.V. Perepelitsa 29,
 E. Perez Codina 166a, M. Perganti 10, L. Perini 68a,68b, H. Pernegger 36, S. Perrella 36, A. Perrevoort 119,
 K. Peters 46, R.F.Y. Peters 100, B.A. Petersen 36, T.C. Petersen 40, E. Petit 101, V. Petousis 140, C. Petridou 161,
 P. Petroff 64, F. Petrucci 74a,74b, M. Pettee 181, N.E. Pettersson 102, K. Petukhova 141, A. Peyaud 143,
 R. Pezoa 145d, L. Pezzotti 70a,70b, G. Pezzullo 181, T. Pham 104, P.W. Phillips 142, M.W. Phipps 171,
 G. Piacquadio 154, E. Pianori 18, F. Piazza 68a,68b, A. Picazio 102, R. Piegaia 30, D. Pietreanu 27b, J.E. Pilcher 37,
 A.D. Pilkington 100, M. Pinamonti 66a,66c, J.L. Pinfold 3, C. Pitman Donaldson 94, D.A. Pizzi 34,
 L. Pizzimento 73a,73b, A. Pizzini 119, M.-A. Pleier 29, V. Plesanovs 52, V. Pleskot 141, E. Plotnikova 79,
 P. Podberezko 121b,121a, R. Poettgen 96, R. Poggi 54, L. Poggioli 134, I. Pogrebnyak 106, D. Pohl 24,
 I. Pokharel 53, G. Polesello 70a, A. Poley 151,166a, A. Pollicchio 72a,72b, R. Polifka 141, A. Polini 23b,
 C.S. Pollard 46, Z.B. Pollock 126, V. Polychronakos 29, D. Ponomarenko 111, L. Pontecorvo 36, S. Popa 27a,
 G.A. Popeneiciu 27d, L. Portales 5, D.M. Portillo Quintero 58, S. Pospisil 140, P. Postolache 27c,
 K. Potamianos 133, I.N. Potrap 79, C.J. Potter 32, H. Potti 11, T. Poulsen 46, J. Poveda 172, T.D. Powell 148,
 G. Pownall 46, M.E. Pozo Astigarraga 36, A. Prades Ibanez 172, P. Pralavorio 101, M.M. Prapa 44, S. Prell 78,
 D. Price 100, M. Primavera 67a, M.A. Principe Martin 98, M.L. Proffitt 147, N. Proklova 111, K. Prokofiev 62c,
 F. Prokoshin 79, S. Protopopescu 29, J. Proudfoot 6, M. Przybycien 83a, D. Pudzha 136, P. Puzo 64,
 D. Pyatiizbyantseva 111, J. Qian 105, Y. Qin 100, A. Quadt 53, M. Queitsch-Maitland 36, G. Rabanal Bolanos 59,
 F. Ragusa 68a,68b, G. Rahal 97, J.A. Raine 54, S. Rajagopalan 29, K. Ran 15a,15d, D.F. Rassloff 61a, D.M. Rauch 46,
 S. Rave 99, B. Ravina 57, I. Ravinovich 178, M. Raymond 36, A.L. Read 132, N.P. Readioff 148, M. Reale 67a,67b,
 D.M. Rebuzzi 70a,70b, G. Redlinger 29, K. Reeves 43, D. Reikher 160, A. Reiss 99, A. Rej 150, C. Rembser 36,
 A. Renardi 46, M. Renda 27b, M.B. Rendel 114, A.G. Rennie 57, S. Resconi 68a, E.D. Resseguei 18, S. Rettie 94,
 B. Reynolds 126, E. Reynolds 21, M. Rezaei Estabragh 180, O.L. Rezanova 121b,121a, P. Reznicek 141,
 E. Ricci 75a,75b, R. Richter 114, S. Richter 46, E. Richter-Was 83b, M. Ridel 134, P. Rieck 114, O. Rifki 46,
 M. Rijssenbeek 154, A. Rimoldi 70a,70b, M. Rimoldi 46, L. Rinaldi 23b, T.T. Rinn 171, M.P. Rinnagel 113,
 G. Ripellino 153, I. Riu 14, P. Rivadeneira 46, J.C. Rivera Vergara 174, F. Rizatdinova 128, E. Rizvi 92, C. Rizzi 54,
 S.H. Robertson 103,aa, M. Robin 46, D. Robinson 32, C.M. Robles Gajardo 145d, M. Robles Manzano 99,
 A. Robson 57, A. Rocchi 73a,73b, C. Roda 71a,71b, S. Rodriguez Bosca 172, A. Rodriguez Rodriguez 52,
 A.M. Rodriguez Vera 166b, S. Roe 36, J. Roggel 180, O. Røhne 132, R.A. Rojas 145d, B. Roland 52,
 C.P.A. Roland 65, J. Roloff 29, A. Romanouk 111, M. Romano 23b,23a, N. Rompotis 90, M. Ronzani 124,
 L. Roos 134, S. Rosati 72a, G. Rosin 102, B.J. Rosser 135, E. Rossi 165, E. Rossi 5, E. Rossi 69a,69b, L.P. Rossi 55b,

- L. Rossini ⁴⁶, R. Rosten ¹²⁶, M. Rotaru ^{27b}, B. Rottler ⁵², D. Rousseau ⁶⁴, D. Roussel ³², G. Rovelli ^{70a,70b},
 A. Roy ¹¹, A. Rozanov ¹⁰¹, Y. Rozen ¹⁵⁹, X. Ruan ^{33f}, A.J. Ruby ⁹⁰, T.A. Ruggeri ¹, F. Rühr ⁵²,
 A. Ruiz-Martinez ¹⁷², A. Rummler ³⁶, Z. Rurikova ⁵², N.A. Rusakovich ⁷⁹, H.L. Russell ³⁶, L. Rustige ³⁸,
 J.P. Rutherford ⁷, E.M. Rüttinger ¹⁴⁸, M. Rybar ¹⁴¹, E.B. Rye ¹³², A. Ryzhov ¹²², J.A. Sabater Iglesias ⁴⁶,
 P. Sabatini ¹⁷², L. Sabetta ^{72a,72b}, H.F-W. Sadrozinski ¹⁴⁴, R. Sadykov ⁷⁹, F. Safai Tehrani ^{72a},
 B. Safarzadeh Samani ¹⁵⁵, M. Safdari ¹⁵², P. Saha ¹²⁰, S. Saha ¹⁰³, M. Sahinsoy ¹¹⁴, A. Sahu ¹⁸⁰,
 M. Saimpert ³⁶, M. Saito ¹⁶², T. Saito ¹⁶², D. Salamani ⁵⁴, G. Salamanna ^{74a,74b}, A. Salnikov ¹⁵², J. Salt ¹⁷²,
 A. Salvador Salas ¹⁴, D. Salvatore ^{41b,41a}, F. Salvatore ¹⁵⁵, A. Salzburger ³⁶, D. Sammel ⁵²,
 D. Sampsonidis ¹⁶¹, D. Sampsonidou ^{60d,60c}, J. Sánchez ¹⁷², A. Sanchez Pineda ^{66a,36,66c}, H. Sandaker ¹³²,
 C.O. Sander ⁴⁶, I.G. Sanderswood ⁸⁹, M. Sandhoff ¹⁸⁰, C. Sandoval ^{22b}, D.P.C. Sankey ¹⁴², M. Sannino ^{55b,55a},
 Y. Sano ¹¹⁶, A. Sansoni ⁵¹, C. Santoni ³⁸, H. Santos ^{138a,138b}, S.N. Santpur ¹⁸, A. Santra ¹⁷⁸, K.A. Saoucha ¹⁴⁸,
 A. Sapronov ⁷⁹, J.G. Saraiva ^{138a,138d}, O. Sasaki ⁸¹, K. Sato ¹⁶⁷, C. Sauer ^{61b}, F. Sauerburger ⁵², E. Sauvan ⁵,
 P. Savard ^{165,ak}, R. Sawada ¹⁶², C. Sawyer ¹⁴², L. Sawyer ⁹⁵, I. Sayago Galvan ¹⁷², C. Sbarra ^{23b},
 A. Sbrizzi ^{66a,66c}, T. Scanlon ⁹⁴, J. Schaarschmidt ¹⁴⁷, P. Schacht ¹¹⁴, D. Schaefer ³⁷, L. Schaefer ¹³⁵,
 U. Schäfer ⁹⁹, A.C. Schaffer ⁶⁴, D. Schaile ¹¹³, R.D. Schamberger ¹⁵⁴, E. Schanet ¹¹³, C. Scharf ¹⁹,
 N. Scharnberg ¹⁰⁰, V.A. Schegelsky ¹³⁶, D. Scheirich ¹⁴¹, F. Schenck ¹⁹, M. Schernau ¹⁶⁹, C. Schiavi ^{55b,55a},
 L.K. Schildgen ²⁴, Z.M. Schillaci ²⁶, E.J. Schioppa ^{67a,67b}, M. Schioppa ^{41b,41a}, B. Schlag ⁹⁹, K.E. Schleicher ⁵²,
 S. Schlenker ³⁶, K. Schmieden ⁹⁹, C. Schmitt ⁹⁹, S. Schmitt ⁴⁶, L. Schoeffel ¹⁴³, A. Schoening ^{61b},
 P.G. Scholer ⁵², E. Schopf ¹³³, M. Schott ⁹⁹, J. Schovancova ³⁶, S. Schramm ⁵⁴, F. Schroeder ¹⁸⁰, A. Schulte ⁹⁹,
 H-C. Schultz-Coulon ^{61a}, M. Schumacher ⁵², B.A. Schumm ¹⁴⁴, Ph. Schune ¹⁴³, A. Schwartzman ¹⁵²,
 T.A. Schwarz ¹⁰⁵, Ph. Schwemling ¹⁴³, R. Schwienhorst ¹⁰⁶, A. Sciandra ¹⁴⁴, G. Sciolla ²⁶, F. Scuri ^{71a},
 F. Scutti ¹⁰⁴, C.D. Sebastiani ⁹⁰, K. Sedlaczek ⁴⁷, P. Seema ¹⁹, S.C. Seidel ¹¹⁷, A. Seiden ¹⁴⁴, B.D. Seidlitz ²⁹,
 T. Seiss ³⁷, C. Seitz ⁴⁶, J.M. Seixas ^{80b}, G. Sekhniaidze ^{69a}, S.J. Sekula ⁴², L.P. Selem ⁵,
 N. Semprini-Cesari ^{23b,23a}, S. Sen ⁴⁹, C. Serfon ²⁹, L. Serin ⁶⁴, L. Serkin ^{66a,66b}, M. Sessa ^{60a}, H. Severini ¹²⁷,
 S. Sevova ¹⁵², F. Sforza ^{55b,55a}, A. Sfyrla ⁵⁴, E. Shabalina ⁵³, J.D. Shahinian ¹³⁵, N.W. Shaikh ^{45a,45b},
 D. Shaked Renous ¹⁷⁸, L.Y. Shan ^{15a}, M. Shapiro ¹⁸, A. Sharma ³⁶, A.S. Sharma ¹, S. Sharma ⁴⁶,
 P.B. Shatalov ¹²³, K. Shaw ¹⁵⁵, S.M. Shaw ¹⁰⁰, M. Shehade ¹⁷⁸, Y. Shen ¹²⁷, P. Sherwood ⁹⁴, L. Shi ⁹⁴,
 C.O. Shimmin ¹⁸¹, Y. Shimogama ¹⁷⁷, M. Shimojima ¹¹⁵, J.D. Shinner ⁹³, I.P.J. Shipsey ¹³³, S. Shirabe ¹⁶³,
 M. Shiyakova ⁷⁹, J. Shlomi ¹⁷⁸, M.J. Shochet ³⁷, J. Shojaii ¹⁰⁴, D.R. Shope ¹⁵³, S. Shrestha ¹²⁶, E.M. Shrif ^{33f},
 M.J. Shroff ¹⁷⁴, E. Shulga ¹⁷⁸, P. Sicho ¹³⁹, A.M. Sickles ¹⁷¹, E. Sideras Haddad ^{33f}, O. Sidiropoulou ³⁶,
 A. Sidoti ^{23b,23a}, F. Siegert ⁴⁸, Dj. Sijacki ¹⁶, M.V. Silva Oliveira ³⁶, S.B. Silverstein ^{45a}, S. Simion ⁶⁴,
 R. Simoniello ³⁶, S. Simsek ^{12b}, P. Sinervo ¹⁶⁵, V. Sinetckii ¹¹², S. Singh ¹⁵¹, S. Sinha ^{33f}, M. Sioli ^{23b,23a},
 I. Siral ¹³⁰, S.Yu. Sivoklokov ¹¹², J. Sjölin ^{45a,45b}, A. Skaf ⁵³, E. Skorda ⁹⁶, P. Skubic ¹²⁷, M. Slawinska ⁸⁴,
 K. Sliwa ¹⁶⁸, V. Smakhtin ¹⁷⁸, B.H. Smart ¹⁴², J. Smiesko ¹⁴¹, S.Yu. Smirnov ¹¹¹, Y. Smirnov ¹¹¹,
 L.N. Smirnova ^{112,s}, O. Smirnova ⁹⁶, E.A. Smith ³⁷, H.A. Smith ¹³³, M. Smizanska ⁸⁹, K. Smolek ¹⁴⁰,
 A. Smykiewicz ⁸⁴, A.A. Snesarev ¹¹⁰, H.L. Snoek ¹¹⁹, I.M. Snyder ¹³⁰, S. Snyder ²⁹, R. Sobie ^{174,aa},
 A. Soffer ¹⁶⁰, A. Søgaard ⁵⁰, F. Sohns ⁵³, C.A. Solans Sanchez ³⁶, E.Yu. Soldatov ¹¹¹, U. Soldevila ¹⁷²,
 A.A. Solodkov ¹²², S. Solomon ⁵², A. Soloshenko ⁷⁹, O.V. Solovyev ¹²², V. Solovyev ¹³⁶, P. Sommer ¹⁴⁸,
 H. Son ¹⁶⁸, A. Sonay ¹⁴, W.Y. Song ^{166b}, A. Sopczak ¹⁴⁰, A.L. Sopio ⁹⁴, F. Sopkova ^{28b}, S. Sottocornola ^{70a,70b},
 R. Soualah ^{66a,66c}, A.M. Soukharev ^{121b,121a}, Z. Soumaimi ^{35f}, D. South ⁴⁶, S. Spagnolo ^{67a,67b}, M. Spalla ¹¹⁴,
 M. Spangenberg ¹⁷⁶, F. Spanò ⁹³, D. Sperlich ⁵², T.M. Spieker ^{61a}, G. Spigo ³⁶, M. Spina ¹⁵⁵, D.P. Spiteri ⁵⁷,
 M. Spousta ¹⁴¹, A. Stabile ^{68a,68b}, B.L. Stamas ¹²⁰, R. Stamen ^{61a}, M. Stamenkovic ¹¹⁹, A. Stampekitis ²¹,
 E. Stanecka ⁸⁴, B. Stanislaus ¹³³, M.M. Stanitzki ⁴⁶, M. Stankaityte ¹³³, B. Stapf ⁴⁶, E.A. Starchenko ¹²²,
 G.H. Stark ¹⁴⁴, J. Stark ¹⁰¹, D.M. Starko ^{166b}, P. Staroba ¹³⁹, P. Starovoitov ^{61a}, S. Stärz ¹⁰³, R. Staszewski ⁸⁴,
 G. Stavropoulos ⁴⁴, P. Steinberg ²⁹, A.L. Steinhebel ¹³⁰, B. Stelzer ^{151,166a}, H.J. Stelzer ¹³⁷,
 O. Stelzer-Chilton ^{166a}, H. Stenzel ⁵⁶, T.J. Stevenson ¹⁵⁵, G.A. Stewart ³⁶, M.C. Stockton ³⁶, G. Stoica ^{27b},
 M. Stolarski ^{138a}, S. Stonjek ¹¹⁴, A. Straessner ⁴⁸, J. Strandberg ¹⁵³, S. Strandberg ^{45a,45b}, M. Strauss ¹²⁷,
 T. Strebler ¹⁰¹, P. Strizenec ^{28b}, R. Ströhmer ¹⁷⁵, D.M. Strom ¹³⁰, L.R. Strom ⁴⁶, R. Stroynowski ⁴²,
 A. Strubig ^{45a,45b}, S.A. Stucci ²⁹, B. Stugu ¹⁷, J. Stupak ¹²⁷, N.A. Styles ⁴⁶, D. Su ¹⁵², S. Su ^{60a},
 W. Su ^{60d,147,60c}, X. Su ^{60a}, N.B. Suarez ¹³⁷, K. Sugizaki ¹⁶², V.V. Sulin ¹¹⁰, M.J. Sullivan ⁹⁰, D.M.S. Sultan ⁵⁴,
 S. Sultansoy ^{4c}, T. Sumida ⁸⁵, S. Sun ¹⁰⁵, S. Sun ¹⁷⁹, X. Sun ¹⁰⁰, C.J.E. Suster ¹⁵⁶, M.R. Sutton ¹⁵⁵,
 M. Svatos ¹³⁹, M. Swiatlowski ^{166a}, S.P. Swift ², T. Swirski ¹⁷⁵, A. Sydorenko ⁹⁹, I. Sykora ^{28a}, M. Sykora ¹⁴¹,
 T. Sykora ¹⁴¹, D. Ta ⁹⁹, K. Tackmann ^{46,y}, A. Taffard ¹⁶⁹, R. Tafirout ^{166a}, E. Tagiev ¹²², R.H.M. Taibah ¹³⁴,

- R. Takashima 86, K. Takeda 82, T. Takeshita 149, E.P. Takeva 50, Y. Takubo 81, M. Talby 101,
 A.A. Talyshov 121b, 121a, K.C. Tam 62b, N.M. Tamir 160, J. Tanaka 162, R. Tanaka 64, S. Tapia Araya 171,
 S. Tapprogge 99, A. Tarek Abouelfadl Mohamed 106, S. Tarem 159, K. Tariq 60b, G. Tarna 27b,f,
 G.F. Tartarelli 68a, P. Tas 141, M. Tasevsky 139, E. Tassi 41b, 41a, G. Tateno 162, Y. Tayalati 35f, G.N. Taylor 104,
 W. Taylor 166b, H. Teagle 90, A.S. Tee 89, R. Teixeira De Lima 152, P. Teixeira-Dias 93, H. Ten Kate 36,
 J.J. Teoh 119, K. Terashi 162, J. Terron 98, S. Terzo 14, M. Testa 51, R.J. Teuscher 165, aa, N. Themistokleous 50,
 T. Theveneaux-Pelzer 19, D.W. Thomas 93, J.P. Thomas 21, E.A. Thompson 46, P.D. Thompson 21,
 E. Thomson 135, E.J. Thorpe 92, Y. Tian 53, V.O. Tikhomirov 110, ag, Yu.A. Tikhonov 121b, 121a,
 S. Timoshenko 111, P. Tipton 181, S. Tisserant 101, S.H. Tlou 33f, A. Tnourji 38, K. Todome 23b, 23a,
 S. Todorova-Nova 141, S. Todt 48, M. Togawa 81, J. Tojo 87, S. Tokár 28a, K. Tokushuku 81, E. Tolley 126,
 R. Tombs 32, M. Tomoto 81, 116, L. Tompkins 152, P. Tornambe 102, E. Torrence 130, H. Torres 48,
 E. Torró Pastor 172, M. Toscani 30, C. Tosciri 37, J. Toth 101, z, D.R. Tovey 148, A. Traeet 17, C.J. Treado 124,
 T. Trefzger 175, A. Tricoli 29, I.M. Trigger 166a, S. Trincaz-Duvold 134, D.A. Trischuk 173, W. Trischuk 165,
 B. Trocmé 58, A. Trofymov 64, C. Troncon 68a, F. Trovato 155, L. Truong 33c, M. Trzebinski 84, A. Trzupek 84,
 F. Tsai 154, A. Tsiamis 161, P.V. Tsiareshka 107, ae, A. Tsirigotis 161, w, V. Tsiskaridze 154, E.G. Tskhadadze 158a,
 M. Tsopoulou 161, I.I. Tsukerman 123, V. Tsulaia 18, S. Tsuno 81, O. Tsur 159, D. Tsybychev 154, Y. Tu 62b,
 A. Tudorache 27b, V. Tudorache 27b, A.N. Tuna 36, S. Turchikhin 79, D. Turgeman 178, I. Turk Cakir 4b, u,
 R.J. Turner 21, R. Turra 68a, P.M. Tuts 39, S. Tzamarias 161, P. Tzanis 10, E. Tzovara 99, K. Uchida 162,
 F. Ukegawa 167, G. Unal 36, M. Unal 11, A. Undrus 29, G. Unel 169, F.C. Ungaro 104, K. Uno 162, J. Urban 28b,
 P. Urquijo 104, G. Usai 8, R. Ushioda 163, Z. Uysal 12d, V. Vacek 140, B. Vachon 103, K.O.H. Vadla 132,
 T. Vafeiadis 36, C. Valderanis 113, E. Valdes Santurio 45a, 45b, M. Valente 166a, S. Valentineti 23b, 23a,
 A. Valero 172, L. Valéry 46, R.A. Vallance 21, A. Vallier 36, J.A. Valls Ferrer 172, T.R. Van Daalen 14,
 P. Van Gemmeren 6, S. Van Stroud 94, I. Van Vulpen 119, M. Vanadia 73a, 73b, W. Vandelli 36,
 M. Vandembroucke 143, E.R. Vandewall 128, D. Vannicola 72a, 72b, L. Vannoli 55b, 55a, R. Vari 72a,
 E.W. Varnes 7, C. Varni 55b, 55a, T. Varol 157, D. Varouchas 64, K.E. Varvell 156, M.E. Vasile 27b, L. Vaslin 38,
 G.A. Vasquez 174, F. Vazeille 38, D. Vazquez Furelos 14, T. Vazquez Schroeder 36, J. Veatch 53, V. Vecchio 100,
 M.J. Veen 119, L.M. Veloce 165, F. Veloso 138a, 138c, S. Veneziano 72a, A. Ventura 67a, 67b, A. Verbytskyi 114,
 M. Verducci 71a, 71b, C. Vergis 24, M. Verissimo De Araujo 80b, W. Verkerke 119, A.T. Vermeulen 119,
 J.C. Vermeulen 119, C. Vernieri 152, P.J. Verschuuren 93, M.L. Vesterbacka 124, M.C. Vetterli 151, ak,
 N. Viaux Maira 145d, T. Vickey 148, O.E. Vickey Boeriu 148, G.H.A. Viehhauser 133, L. Vigani 61b,
 M. Villa 23b, 23a, M. Villaplana Perez 172, E.M. Villhauer 50, E. Vilucchi 51, M.G. Vincter 34, G.S. Virdee 21,
 A. Vishwakarma 50, C. Vittori 23b, 23a, I. Vivarelli 155, V. Vladimirov 176, M. Vogel 180, P. Vokac 140,
 J. Von Ahnen 46, S.E. von Buddenbrock 33f, E. Von Toerne 24, V. Vorobel 141, K. Vorobev 111, M. Vos 172,
 J.H. Vossebeld 90, M. Vozak 100, N. Vranjes 16, M. Vranjes Milosavljevic 16, V. Vrba 140, *, M. Vreeswijk 119,
 N.K. Vu 101, R. Vuillermet 36, I. Vukotic 37, S. Wada 167, C. Wagner 102, P. Wagner 24, W. Wagner 180,
 S. Wahdan 180, H. Wahlberg 88, R. Wakasa 167, M. Wakida 116, V.M. Walbrecht 114, J. Walder 142,
 R. Walker 113, S.D. Walker 93, W. Walkowiak 150, V. Wallangen 45a, 45b, A.M. Wang 59, A.Z. Wang 179,
 C. Wang 60a, C. Wang 60c, H. Wang 18, J. Wang 62a, P. Wang 42, R.-J. Wang 99, R. Wang 59, R. Wang 120,
 S.M. Wang 157, S. Wang 60b, T. Wang 60a, W.T. Wang 60a, W.X. Wang 60a, X. Wang 171, Y. Wang 60a,
 Z. Wang 105, C. Wanotayaroj 36, A. Warburton 103, C.P. Ward 32, R.J. Ward 21, N. Warrack 57, A.T. Watson 21,
 M.F. Watson 21, G. Watts 147, B.M. Waugh 94, A.F. Webb 11, C. Weber 29, M.S. Weber 20, S.A. Weber 34,
 S.M. Weber 61a, C. Wei 60a, Y. Wei 133, A.R. Weidberg 133, J. Weingarten 47, M. Weirich 99, C. Weiser 52,
 P.S. Wells 36, T. Wenaus 29, B. Wendland 47, T. Wengler 36, S. Wenig 36, N. Wermes 24, M. Wessels 61a,
 T.D. Weston 20, K. Whalen 130, A.M. Wharton 89, A.S. White 59, A. White 8, M.J. White 1, D. Whiteson 169,
 W. Wiedenmann 179, C. Wiel 48, M. Wielers 142, N. Wieseotte 99, C. Wiglesworth 40, L.A.M. Wiik-Fuchs 52,
 H.G. Wilkens 36, L.J. Wilkins 93, D.M. Williams 39, H.H. Williams 135, S. Williams 32, S. Willocq 102,
 P.J. Windischhofer 133, I. Wingerter-Seez 5, F. Winklmeier 130, B.T. Winter 52, M. Wittgen 152,
 M. Wobisch 95, A. Wolf 99, R. Wölker 133, J. Wollrath 52, M.W. Wolter 84, H. Wolters 138a, 138c,
 V.W.S. Wong 173, A.F. Wongel 46, N.L. Woods 144, S.D. Worm 46, B.K. Wosiek 84, K.W. Woźniak 84,
 K. Wright 57, J. Wu 15a, 15d, S.L. Wu 179, X. Wu 54, Y. Wu 60a, Z. Wu 143, J. Wuerzinger 133, T.R. Wyatt 100,
 B.M. Wynne 50, S. Xella 40, J. Xiang 62c, X. Xiao 105, X. Xie 60a, I. Xiotidis 155, D. Xu 15a, H. Xu 60a, H. Xu 60a,
 L. Xu 60a, R. Xu 135, W. Xu 105, Y. Xu 15b, Z. Xu 60b, Z. Xu 152, B. Yabsley 156, S. Yacoob 33a, D.P. Yallup 94,
 N. Yamaguchi 87, Y. Yamaguchi 163, M. Yamatani 162, H. Yamauchi 167, T. Yamazaki 18, Y. Yamazaki 82,

J. Yan ^{60c}, Z. Yan ²⁵, H.J. Yang ^{60c,60d}, H.T. Yang ¹⁸, S. Yang ^{60a}, T. Yang ^{62c}, X. Yang ^{60a}, X. Yang ^{15a}, Y. Yang ¹⁶², Z. Yang ^{105,60a}, W-M. Yao ¹⁸, Y.C. Yap ⁴⁶, H. Ye ^{15c}, J. Ye ⁴², S. Ye ²⁹, I. Yeletskikh ⁷⁹, M.R. Yexley ⁸⁹, P. Yin ³⁹, K. Yorita ¹⁷⁷, K. Yoshihara ⁷⁸, C.J.S. Young ³⁶, C. Young ¹⁵², R. Yuan ^{60b,j}, X. Yue ^{61a}, M. Zaazoua ^{35f}, B. Zabinski ⁸⁴, G. Zacharis ¹⁰, E. Zaffaroni ⁵⁴, J. Zahreddine ¹⁰¹, A.M. Zaitsev ^{122,af}, T. Zakareishvili ^{158b}, N. Zakharchuk ³⁴, S. Zambito ³⁶, D. Zanzi ⁵², S.V. Zeißner ⁴⁷, C. Zeitnitz ¹⁸⁰, G. Zemaityte ¹³³, J.C. Zeng ¹⁷¹, O. Zenin ¹²², T. Ženiš ^{28a}, S. Zenz ⁹², S. Zerradi ^{35a}, D. Zerwas ⁶⁴, M. Zgubić ¹³³, B. Zhang ^{15c}, D.F. Zhang ^{15b}, G. Zhang ^{15b}, J. Zhang ⁶, K. Zhang ^{15a}, L. Zhang ^{15c}, M. Zhang ¹⁷¹, R. Zhang ¹⁷⁹, S. Zhang ¹⁰⁵, X. Zhang ^{60c}, X. Zhang ^{60b}, Z. Zhang ⁶⁴, P. Zhao ⁴⁹, Y. Zhao ¹⁴⁴, Z. Zhao ^{60a}, A. Zhemchugov ⁷⁹, Z. Zheng ¹⁰⁵, D. Zhong ¹⁷¹, B. Zhou ¹⁰⁵, C. Zhou ¹⁷⁹, H. Zhou ⁷, M. Zhou ¹⁵⁴, N. Zhou ^{60c}, Y. Zhou ⁷, C.G. Zhu ^{60b}, C. Zhu ^{15a,15d}, H.L. Zhu ^{60a}, H. Zhu ^{15a}, J. Zhu ¹⁰⁵, Y. Zhu ^{60a}, X. Zhuang ^{15a}, K. Zhukov ¹¹⁰, V. Zhulanov ^{121b,121a}, D. Ziemińska ⁶⁵, N.I. Zimine ⁷⁹, S. Zimmermann ^{52,*}, Z. Zinonos ¹¹⁴, M. Ziolkowski ¹⁵⁰, L. Živković ¹⁶, A. Zoccoli ^{23b,23a}, K. Zoch ⁵³, T.G. Zorbas ¹⁴⁸, R. Zou ³⁷, W. Zou ³⁹, L. Zwaliński ³⁶

¹ Department of Physics, University of Adelaide, Adelaide, Australia² Physics Department, SUNY Albany, Albany NY, United States of America³ Department of Physics, University of Alberta, Edmonton AB, Canada⁴ ^(a) Department of Physics, Ankara University, Ankara; ^(b) Istanbul Aydin University, Application and Research Center for Advanced Studies, Istanbul; ^(c) Division of Physics, TOBB University of Economics and Technology, Ankara, Turkey⁵ LAPP, Univ. Savoie Mont Blanc, CNRS/IN2P3, Annecy, France⁶ High Energy Physics Division, Argonne National Laboratory, Argonne IL, United States of America⁷ Department of Physics, University of Arizona, Tucson AZ, United States of America⁸ Department of Physics, University of Texas at Arlington, Arlington TX, United States of America⁹ Physics Department, National and Kapodistrian University of Athens, Athens, Greece¹⁰ Physics Department, National Technical University of Athens, Zografou, Greece¹¹ Department of Physics, University of Texas at Austin, Austin TX, United States of America¹² ^(a) Bahçeşehir University, Faculty of Engineering and Natural Sciences, Istanbul; ^(b) İstanbul Bilgi University, Faculty of Engineering and Natural Sciences, Istanbul; ^(c) Department of Physics, Bogazici University, Istanbul; ^(d) Department of Physics Engineering, Gaziantep University, Gaziantep, Turkey¹³ Institute of Physics, Azerbaijan Academy of Sciences, Baku, Azerbaijan¹⁴ Institut de Física d'Altes Energies (IFAE), Barcelona Institute of Science and Technology, Barcelona, Spain¹⁵ ^(a) Institute of High Energy Physics, Chinese Academy of Sciences, Beijing; ^(b) Physics Department, Tsinghua University, Beijing; ^(c) Department of Physics, Nanjing University, Nanjing;^(d) University of Chinese Academy of Science (UCAS), Beijing, China¹⁶ Institute of Physics, University of Belgrade, Belgrade, Serbia¹⁷ Department for Physics and Technology, University of Bergen, Bergen, Norway¹⁸ Physics Division, Lawrence Berkeley National Laboratory and University of California, Berkeley CA, United States of America¹⁹ Institut für Physik, Humboldt Universität zu Berlin, Berlin, Germany²⁰ Albert Einstein Center for Fundamental Physics and Laboratory for High Energy Physics, University of Bern, Bern, Switzerland²¹ School of Physics and Astronomy, University of Birmingham, Birmingham, United Kingdom²² ^(a) Facultad de Ciencias y Centro de Investigaciones, Universidad Antonio Narino, Bogotá; ^(b) Departamento de Física, Universidad Nacional de Colombia, Bogotá, Colombia, Colombia²³ ^(a) INFN Bologna and Università di Bologna, Dipartimento di Fisica; ^(b) INFN Sezione di Bologna, Italy²⁴ Physikalisches Institut, Universität Bonn, Bonn, Germany²⁵ Department of Physics, Boston University, Boston MA, United States of America²⁶ Department of Physics, Brandeis University, Waltham MA, United States of America²⁷ ^(a) Transilvania University of Brasov, Brasov; ^(b) Horia Hulubei National Institute of Physics and Nuclear Engineering, Bucharest; ^(c) Department of Physics, Alexandru Ioan Cuza University of Iasi, Iasi; ^(d) National Institute for Research and Development of Isotopic and Molecular Technologies, Physics Department, Cluj-Napoca; ^(e) University Politehnica Bucharest, Bucharest; ^(f) West University in Timisoara, Timisoara, Romania²⁸ ^(a) Faculty of Mathematics, Physics and Informatics, Comenius University, Bratislava; ^(b) Department of Subnuclear Physics, Institute of Experimental Physics of the Slovak Academy of Sciences, Košice, Slovak Republic²⁹ Physics Department, Brookhaven National Laboratory, Upton NY, United States of America³⁰ Departamento de Física, Universidad de Buenos Aires, Buenos Aires, Argentina³¹ California State University, CA, United States of America³² Cavendish Laboratory, University of Cambridge, Cambridge, United Kingdom³³ ^(a) Department of Physics, University of Cape Town, Cape Town; ^(b) iThemba Labs, Western Cape; ^(c) Department of Mechanical Engineering Science, University of Johannesburg, Johannesburg; ^(d) National Institute of Physics, University of the Philippines Diliman; ^(e) University of South Africa, Department of Physics, Pretoria; ^(f) School of Physics, University of the Witwatersrand, Johannesburg, South Africa³⁴ Department of Physics, Carleton University, Ottawa ON, Canada³⁵ ^(a) Faculté des Sciences Ain Chock, Réseau Universitaire de Physique des Hautes Energies – Université Hassan II, Casablanca; ^(b) Faculté des Sciences, Université Ibn-Tofail, Kénitra;^(c) Faculté des Sciences Semlalia, Université Cadi Ayyad, LPHEA, Marrakech; ^(d) Moroccan Foundation for Advanced Science Innovation and Research (MASCIIR), Rabat; ^(e) LPMR, Faculté des Sciences, Université Mohamed Premier, Oujda; ^(f) Faculté des sciences, Université Mohammed V, Rabat, Morocco³⁶ CERN, Geneva, Switzerland³⁷ Enrico Fermi Institute, University of Chicago, Chicago IL, United States of America³⁸ LPC, Université Clermont Auvergne, CNRS/IN2P3, Clermont-Ferrand, France³⁹ Nevis Laboratory, Columbia University, Irvington NY, United States of America⁴⁰ Niels Bohr Institute, University of Copenhagen, Copenhagen, Denmark⁴¹ ^(a) Dipartimento di Fisica, Università della Calabria, Rende; ^(b) INFN Gruppo Collegato di Cosenza, Laboratori Nazionali di Frascati, Italy⁴² Physics Department, Southern Methodist University, Dallas TX, United States of America⁴³ Physics Department, University of Texas at Dallas, Richardson TX, United States of America⁴⁴ National Centre for Scientific Research "Demokritos", Agia Paraskevi, Greece⁴⁵ ^(a) Department of Physics, Stockholm University; ^(b) Oskar Klein Centre, Stockholm, Sweden⁴⁶ Deutsches Elektronen-Synchrotron DESY, Hamburg and Zeuthen, Germany⁴⁷ Lehrstuhl für Experimentelle Physik IV, Technische Universität Dortmund, Dortmund, Germany⁴⁸ Institut für Kern- und Teilchenphysik, Technische Universität Dresden, Dresden, Germany⁴⁹ Department of Physics, Duke University, Durham NC, United States of America⁵⁰ SUPA – School of Physics and Astronomy, University of Edinburgh, Edinburgh, United Kingdom

- ⁵¹ INFN e Laboratori Nazionali di Frascati, Frascati, Italy
⁵² Physikalisches Institut, Albert-Ludwigs-Universität Freiburg, Freiburg, Germany
⁵³ II. Physikalisches Institut, Georg-August-Universität Göttingen, Göttingen, Germany
⁵⁴ Département de Physique Nucléaire et Corpusculaire, Université de Genève, Genève, Switzerland
⁵⁵ ^(a) Dipartimento di Fisica, Università di Genova, Genova; ^(b) INFN Sezione di Genova, Italy
⁵⁶ II. Physikalisches Institut, Justus-Liebig-Universität Giessen, Giessen, Germany
⁵⁷ SUPA – School of Physics and Astronomy, University of Glasgow, Glasgow, United Kingdom
⁵⁸ LPSC, Université Grenoble Alpes, CNRS/IN2P3, Grenoble INP, Grenoble, France
⁵⁹ Laboratory for Particle Physics and Cosmology, Harvard University, Cambridge MA, United States of America
⁶⁰ ^(a) Department of Modern Physics and State Key Laboratory of Particle Detection and Electronics, University of Science and Technology of China, Hefei; ^(b) Institute of Frontier and Interdisciplinary Science and Key Laboratory of Particle Physics and Particle Irradiation (MOE), Shandong University, Qingdao; ^(c) School of Physics and Astronomy, Shanghai Jiao Tong University, Key Laboratory for Particle Astrophysics and Cosmology (MOE), SKLPPC, Shanghai; ^(d) Tsung-Dao Lee Institute, Shanghai, China
⁶¹ ^(a) Kirchhoff-Institut für Physik, Ruprecht-Karls-Universität Heidelberg, Heidelberg; ^(b) Physikalisches Institut, Ruprecht-Karls-Universität Heidelberg, Heidelberg, Germany
⁶² ^(a) Department of Physics, Chinese University of Hong Kong, Shatin, N.T., Hong Kong; ^(b) Department of Physics, University of Hong Kong, Hong Kong; ^(c) Department of Physics and Institute for Advanced Study, Hong Kong University of Science and Technology, Clear Water Bay, Kowloon, Hong Kong, China
⁶³ Department of Physics, National Tsing Hua University, Hsinchu, Taiwan
⁶⁴ IJCLab, Université Paris-Saclay, CNRS/IN2P3, 91405, Orsay, France
⁶⁵ Department of Physics, Indiana University, Bloomington IN, United States of America
⁶⁶ ^(a) INFN Gruppo Collegato di Udine, Sezione di Trieste, Udine; ^(b) ICTP, Trieste; ^(c) Dipartimento Politecnico di Ingegneria e Architettura, Università di Udine, Udine, Italy
⁶⁷ ^(a) INFN Sezione di Lecce; ^(b) Dipartimento di Matematica e Fisica, Università del Salento, Lecce, Italy
⁶⁸ ^(a) INFN Sezione di Milano; ^(b) Dipartimento di Fisica, Università di Milano, Milano, Italy
⁶⁹ ^(a) INFN Sezione di Napoli; ^(b) Dipartimento di Fisica, Università di Napoli, Napoli, Italy
⁷⁰ ^(a) INFN Sezione di Pavia; ^(b) Dipartimento di Fisica, Università di Pavia, Pavia, Italy
⁷¹ ^(a) INFN Sezione di Pisa; ^(b) Dipartimento di Fisica E. Fermi, Università di Pisa, Pisa, Italy
⁷² ^(a) INFN Sezione di Roma; ^(b) Dipartimento di Fisica, Sapienza Università di Roma, Roma, Italy
⁷³ ^(a) INFN Sezione di Roma Tor Vergata; ^(b) Dipartimento di Fisica, Università di Roma Tor Vergata, Roma, Italy
⁷⁴ ^(a) INFN Sezione di Roma Tre; ^(b) Dipartimento di Matematica e Fisica, Università Roma Tre, Roma, Italy
⁷⁵ ^(a) INFN-TIFPA; ^(b) Università degli Studi di Trento, Trento, Italy
⁷⁶ Institut für Astro- und Teilchenphysik, Leopold-Franzens-Universität, Innsbruck, Austria
⁷⁷ University of Iowa, Iowa City IA, United States of America
⁷⁸ Department of Physics and Astronomy, Iowa State University, Ames IA, United States of America
⁷⁹ Joint Institute for Nuclear Research, Dubna, Russia
⁸⁰ ^(a) Departamento de Engenharia Elétrica, Universidade Federal de Juiz de Fora (UFJF), Juiz de Fora; ^(b) Universidade Federal do Rio De Janeiro COPPE/EE/IF, Rio de Janeiro; ^(c) Instituto de Física, Universidade de São Paulo, São Paulo, Brazil
⁸¹ KEK, High Energy Accelerator Research Organization, Tsukuba, Japan
⁸² Graduate School of Science, Kobe University, Kobe, Japan
⁸³ ^(a) AGH University of Science and Technology, Faculty of Physics and Applied Computer Science, Krakow; ^(b) Marian Smoluchowski Institute of Physics, Jagiellonian University, Krakow, Poland
⁸⁴ Institute of Nuclear Physics Polish Academy of Sciences, Krakow, Poland
⁸⁵ Faculty of Science, Kyoto University, Kyoto, Japan
⁸⁶ Kyoto University of Education, Kyoto, Japan
⁸⁷ Research Center for Advanced Particle Physics and Department of Physics, Kyushu University, Fukuoka, Japan
⁸⁸ Instituto de Física La Plata, Universidad Nacional de La Plata and CONICET, La Plata, Argentina
⁸⁹ Physics Department, Lancaster University, Lancaster, United Kingdom
⁹⁰ Oliver Lodge Laboratory, University of Liverpool, Liverpool, United Kingdom
⁹¹ Department of Experimental Particle Physics, Jožef Stefan Institute and Department of Physics, University of Ljubljana, Ljubljana, Slovenia
⁹² School of Physics and Astronomy, Queen Mary University of London, London, United Kingdom
⁹³ Department of Physics, Royal Holloway University of London, Egham, United Kingdom
⁹⁴ Department of Physics and Astronomy, University College London, London, United Kingdom
⁹⁵ Louisiana Tech University, Ruston LA, United States of America
⁹⁶ Fysiska institutionen, Lunds universitet, Lund, Sweden
⁹⁷ Centre de Calcul de l'Institut National de Physique Nucléaire et de Physique des Particules (IN2P3), Villeurbanne, France
⁹⁸ Departamento de Física Teórica C-15 and CIAFF, Universidad Autónoma de Madrid, Madrid, Spain
⁹⁹ Institut für Physik, Universität Mainz, Mainz, Germany
¹⁰⁰ School of Physics and Astronomy, University of Manchester, Manchester, United Kingdom
¹⁰¹ CPPM, Aix-Marseille Université, CNRS/IN2P3, Marseille, France
¹⁰² Department of Physics, University of Massachusetts, Amherst MA, United States of America
¹⁰³ Department of Physics, McGill University, Montreal QC, Canada
¹⁰⁴ School of Physics, University of Melbourne, Victoria, Australia
¹⁰⁵ Department of Physics, University of Michigan, Ann Arbor MI, United States of America
¹⁰⁶ Department of Physics and Astronomy, Michigan State University, East Lansing MI, United States of America
¹⁰⁷ B.I. Stepanov Institute of Physics, National Academy of Sciences of Belarus, Minsk, Belarus
¹⁰⁸ Research Institute for Nuclear Problems of Byelorussian State University, Minsk, Belarus
¹⁰⁹ Group of Particle Physics, University of Montreal, Montreal QC, Canada
¹¹⁰ P.N. Lebedev Physical Institute of the Russian Academy of Sciences, Moscow, Russia
¹¹¹ National Research Nuclear University MEPhI, Moscow, Russia
¹¹² D.V. Skobeltsyn Institute of Nuclear Physics, M.V. Lomonosov Moscow State University, Moscow, Russia
¹¹³ Fakultät für Physik, Ludwig-Maximilians-Universität München, München, Germany
¹¹⁴ Max-Planck-Institut für Physik (Werner-Heisenberg-Institut), München, Germany
¹¹⁵ Nagasaki Institute of Applied Science, Nagasaki, Japan
¹¹⁶ Graduate School of Science and Kobayashi-Maskawa Institute, Nagoya University, Nagoya, Japan
¹¹⁷ Department of Physics and Astronomy, University of New Mexico, Albuquerque NM, United States of America
¹¹⁸ Institute for Mathematics, Astrophysics and Particle Physics, Radboud University/Nikhef, Nijmegen, Netherlands
¹¹⁹ Nikhef National Institute for Subatomic Physics and University of Amsterdam, Amsterdam, Netherlands
¹²⁰ Department of Physics, Northern Illinois University, DeKalb IL, United States of America
¹²¹ ^(a) Budker Institute of Nuclear Physics and NSU, SB RAS, Novosibirsk; ^(b) Novosibirsk State University Novosibirsk, Russia
¹²² Institute for High Energy Physics of the National Research Centre Kurchatov Institute, Protvino, Russia
¹²³ Institute for Theoretical and Experimental Physics named by A.I. Alikhanov of National Research Centre "Kurchatov Institute", Moscow, Russia
¹²⁴ Department of Physics, New York University, New York NY, United States of America
¹²⁵ Ochanomizu University, Otsuka, Bunkyo-ku, Tokyo, Japan

- ¹²⁶ Ohio State University, Columbus OH, United States of America
¹²⁷ Homer L. Dodge Department of Physics and Astronomy, University of Oklahoma, Norman OK, United States of America
¹²⁸ Department of Physics, Oklahoma State University, Stillwater OK, United States of America
¹²⁹ Palacký University, RCPTM, Joint Laboratory of Optics, Olomouc, Czech Republic
¹³⁰ Institute for Fundamental Science, University of Oregon, Eugene, OR, United States of America
¹³¹ Graduate School of Science, Osaka University, Osaka, Japan
¹³² Department of Physics, University of Oslo, Oslo, Norway
¹³³ Department of Physics, Oxford University, Oxford, United Kingdom
¹³⁴ LPNHE, Sorbonne Université, Université de Paris, CNRS/IN2P3, Paris, France
¹³⁵ Department of Physics, University of Pennsylvania, Philadelphia PA, United States of America
¹³⁶ Konstantinov Nuclear Physics Institute of National Research Centre "Kurchatov Institute", PNPI, St. Petersburg, Russia
¹³⁷ Department of Physics and Astronomy, University of Pittsburgh, Pittsburgh PA, United States of America
¹³⁸ ^(a) Laboratório de Instrumentação e Física Experimental de Partículas – LIP, Lisboa; ^(b) Departamento de Física, Faculdade de Ciências, Universidade de Lisboa, Lisboa; ^(c) Departamento de Física, Universidade de Coimbra, Coimbra; ^(d) Centro de Física Nuclear da Universidade de Lisboa, Lisboa; ^(e) Departamento de Física, Universidade do Minho, Braga; ^(f) Departamento de Física Teórica y del Cosmos, Universidad de Granada, Granada (Spain); ^(g) Dep Física and CEFITEC of Faculdade de Ciências e Tecnologia, Universidade Nova de Lisboa, Caparica;
^(h) Instituto Superior Técnico, Universidade de Lisboa, Lisboa, Portugal
¹³⁹ Institute of Physics of the Czech Academy of Sciences, Prague, Czech Republic
¹⁴⁰ Czech Technical University in Prague, Prague, Czech Republic
¹⁴¹ Charles University, Faculty of Mathematics and Physics, Prague, Czech Republic
¹⁴² Particle Physics Department, Rutherford Appleton Laboratory, Didcot, United Kingdom
¹⁴³ IRFU, CEA, Université Paris-Saclay, Gif-sur-Yvette, France
¹⁴⁴ Santa Cruz Institute for Particle Physics, University of California Santa Cruz, Santa Cruz CA, United States of America
¹⁴⁵ ^(a) Departamento de Física, Pontificia Universidad Católica de Chile, Santiago; ^(b) Universidad Andres Bello, Department of Physics, Santiago; ^(c) Instituto de Alta Investigación, Universidad de Tarapacá; ^(d) Departamento de Física, Universidad Técnica Federico Santa María, Valparaíso, Chile
¹⁴⁶ Universidade Federal de São João del Rei (UFSJ), São João del Rei, Brazil
¹⁴⁷ Department of Physics, University of Washington, Seattle WA, United States of America
¹⁴⁸ Department of Physics and Astronomy, University of Sheffield, Sheffield, United Kingdom
¹⁴⁹ Department of Physics, Shinshu University, Nagano, Japan
¹⁵⁰ Department Physik, Universität Siegen, Siegen, Germany
¹⁵¹ Department of Physics, Simon Fraser University, Burnaby BC, Canada
¹⁵² SLAC National Accelerator Laboratory, Stanford CA, United States of America
¹⁵³ Physics Department, Royal Institute of Technology, Stockholm, Sweden
¹⁵⁴ Departments of Physics and Astronomy, Stony Brook University, Stony Brook NY, United States of America
¹⁵⁵ Department of Physics and Astronomy, University of Sussex, Brighton, United Kingdom
¹⁵⁶ School of Physics, University of Sydney, Sydney, Australia
¹⁵⁷ Institute of Physics, Academia Sinica, Taipei, Taiwan
¹⁵⁸ ^(a) E. Andronikashvili Institute of Physics, Iv. Javakhishvili Tbilisi State University, Tbilisi; ^(b) High Energy Physics Institute, Tbilisi State University, Tbilisi, Georgia
¹⁵⁹ Department of Physics, Technion, Israel Institute of Technology, Haifa, Israel
¹⁶⁰ Raymond and Beverly Sackler School of Physics and Astronomy, Tel Aviv University, Tel Aviv, Israel
¹⁶¹ Department of Physics, Aristotle University of Thessaloniki, Thessaloniki, Greece
¹⁶² International Center for Elementary Particle Physics and Department of Physics, University of Tokyo, Tokyo, Japan
¹⁶³ Department of Physics, Tokyo Institute of Technology, Tokyo, Japan
¹⁶⁴ Tomsk State University, Tomsk, Russia
¹⁶⁵ Department of Physics, University of Toronto, Toronto ON, Canada
¹⁶⁶ ^(a) TRIUMF, Vancouver BC; ^(b) Department of Physics and Astronomy, York University, Toronto ON, Canada
¹⁶⁷ Division of Physics and Tomonaga Center for the History of the Universe, Faculty of Pure and Applied Sciences, University of Tsukuba, Tsukuba, Japan
¹⁶⁸ Department of Physics and Astronomy, Tufts University, Medford MA, United States of America
¹⁶⁹ Department of Physics and Astronomy, University of California Irvine, Irvine CA, United States of America
¹⁷⁰ Department of Physics and Astronomy, University of Uppsala, Uppsala, Sweden
¹⁷¹ Department of Physics, University of Illinois, Urbana IL, United States of America
¹⁷² Instituto de Física Corpuscular (IFIC), Centro Mixto Universidad de Valencia – CSIC, Valencia, Spain
¹⁷³ Department of Physics, University of British Columbia, Vancouver BC, Canada
¹⁷⁴ Department of Physics and Astronomy, University of Victoria, Victoria BC, Canada
¹⁷⁵ Fakultät für Physik und Astronomie, Julius-Maximilians-Universität Würzburg, Würzburg, Germany
¹⁷⁶ Department of Physics, University of Warwick, Coventry, United Kingdom
¹⁷⁷ Waseda University, Tokyo, Japan
¹⁷⁸ Department of Particle Physics and Astrophysics, Weizmann Institute of Science, Rehovot, Israel
¹⁷⁹ Department of Physics, University of Wisconsin, Madison WI, United States of America
¹⁸⁰ Fakultät für Mathematik und Naturwissenschaften, Fachgruppe Physik, Bergische Universität Wuppertal, Wuppertal, Germany
¹⁸¹ Department of Physics, Yale University, New Haven CT, United States of America

^a Also at Borough of Manhattan Community College, City University of New York, New York NY, United States of America.^b Also at Bruno Kessler Foundation, Trento, Italy.^c Also at Center for High Energy Physics, Peking University, China.^d Also at Centro Studi e Ricerche Enrico Fermi, Italy.^e Also at CERN, Geneva, Switzerland.^f Also at CPPM, Aix-Marseille Université, CNRS/IN2P3, Marseille, France.^g Also at Département de Physique Nucléaire et Corpusculaire, Université de Genève, Genève, Switzerland.^h Also at Departament de Fisica de la Universitat Autònoma de Barcelona, Barcelona, Spain.ⁱ Also at Department of Financial and Management Engineering, University of the Aegean, Chios, Greece.^j Also at Department of Physics and Astronomy, Michigan State University, East Lansing MI, United States of America.^k Also at Department of Physics and Astronomy, University of Louisville, Louisville, KY, United States of America.^l Also at Department of Physics, Ben Gurion University of the Negev, Beer Sheva, Israel.^m Also at Department of Physics, California State University, East Bay, United States of America.ⁿ Also at Department of Physics, California State University, Fresno, United States of America.^o Also at Department of Physics, California State University, Sacramento, United States of America.^p Also at Department of Physics, King's College London, London, United Kingdom.^q Also at Department of Physics, St. Petersburg State Polytechnical University, St. Petersburg, Russia.

- ^r Also at Department of Physics, University of Fribourg, Fribourg, Switzerland.
^s Also at Faculty of Physics, M.V. Lomonosov Moscow State University, Moscow, Russia.
^t Also at Faculty of Physics, Sofia University, 'St. Kliment Ohridski', Sofia, Bulgaria.
^u Also at Giresun University, Faculty of Engineering, Giresun, Turkey.
^v Also at Graduate School of Science, Osaka University, Osaka, Japan.
^w Also at Hellenic Open University, Patras, Greece.
^x Also at Institutio Catalana de Recerca i Estudis Avancats, ICREA, Barcelona, Spain.
^y Also at Institut für Experimentalphysik, Universität Hamburg, Hamburg, Germany.
^z Also at Institute for Particle and Nuclear Physics, Wigner Research Centre for Physics, Budapest, Hungary.
^{aa} Also at Institute of Particle Physics (IPP), Canada.
^{ab} Also at Institute of Physics, Azerbaijan Academy of Sciences, Baku, Azerbaijan.
^{ac} Also at Instituto de Fisica Teorica, IFT-UAM/CSIC, Madrid, Spain.
^{ad} Also at Istanbul University, Dept. of Physics, Istanbul, Turkey.
^{ae} Also at Joint Institute for Nuclear Research, Dubna, Russia.
^{af} Also at Moscow Institute of Physics and Technology State University, Dolgoprudny, Russia.
^{ag} Also at National Research Nuclear University MEPhI, Moscow, Russia.
^{ah} Also at Physics Department, An-Najah National University, Nablus, Palestine.
^{ai} Also at Physikalischs Institut, Albert-Ludwigs-Universität Freiburg, Freiburg, Germany.
^{aj} Also at The City College of New York, New York NY, United States of America.
^{ak} Also at TRIUMF, Vancouver BC, Canada.
^{al} Also at Universita di Napoli Parthenope, Napoli, Italy.
^{am} Also at University of Chinese Academy of Sciences (UCAS), Beijing, China.
- * Deceased.